

SYNTHESIS AND CHARACTERIZATION OF SEMICONDUCTOR THIN  
FILMS FOR PHOTOVOLTAIC APPLICATIONS

A THESIS SUBMITTED TO  
THE GRADUATE SCHOOL OF NATURAL AND APPLIED SCIENCES  
OF  
MIDDLE EAST TECHNICAL UNIVERSITY

BY

TAMER TEZEL

IN PARTIAL FULFILLMENT OF THE REQUIREMENTS  
FOR THE DEGREE OF  
MASTER OF SCIENCE  
IN  
CHEMISTRY

SEPTEMBER 2009

Approval of the thesis:

**SYNTHESIS AND CHARACTERIZATION OF SEMICONDUCTOR THIN FILMS FOR PHOTOVOLTAIC APPLICATIONS**

submitted by **TAMER TEZEL** in partial fulfillment of the requirements for the degree of **Master of Science in Department of Chemistry, Middle East Technical University** by,

Prof. Dr. Canan Özgen \_\_\_\_\_  
Dean, Graduate School of **Natural and Applied Sciences**

Prof. Dr. Ahmet M. Önal \_\_\_\_\_  
Head of Department, **Chemistry Dept., METU**

Prof. Dr. Zuhâl Küçükyavuz \_\_\_\_\_  
Supervisor, **Chemistry Dept., METU**

Assoc. Prof. Dr. Nurdan D. Sankır \_\_\_\_\_  
Co-advisor, **Physics Dept., TOBB-ETU**

**Examining Committee Members:**

Prof. Dr. Erdal Bayramlı \_\_\_\_\_  
Chemistry Dept., METU

Prof. Dr. Zuhâl Küçükyavuz \_\_\_\_\_  
Chemistry Dept., METU

Prof. Dr. Ahmet M. Önal \_\_\_\_\_  
Chemistry Dept., METU

Prof. Dr. Mehmet Parlak \_\_\_\_\_  
Physics Dept., METU

Assoc. Prof. Dr. Nurdan D. Sankır \_\_\_\_\_  
Physics Dept., TOBB-ETU

**Date:** 07.09.2009

**I hereby declare that all information in this document has been obtained and presented in accordance with academic rules and ethical conduct. I also declare that, as required by these rules and conduct, I have fully cited and referenced all material and results that are not original to this work.**

Name, Last Name: Tamer Tezel

Signature:

## **ABSTRACT**

### **SYNTHESIS AND CHARACTERIZATION OF SEMICONDUCTOR THIN FILMS FOR PHOTOVOLTAIC APPLICATIONS**

Tezel, Tamer

M.Sc., Department of Chemistry

Supervisor: Prof. Dr. Zuhal Kucukyavuz

Co-supervisor: Assoc. Prof. Dr. Nurdan Demirci Sankır

September 2009, 70 pages

Cadmium sulfide (CdS) thin films are very attractive materials due to their tunable optical properties and potential applications in not only photovoltaic devices but also in electronics, bio-labeling and fluorescence imaging. Recently, there is a great interest in flexible photovoltaic devices due to their unique properties such as very low weight, mechanical durability and large area applications. Organic semiconductors and their heterojunctions with inorganic materials are the most promising candidates for flexible photovoltaic applications. Preparation of CdS and Polypyrrole (PPy) semiconducting thin films on flexible polyethyleneterephthalate (PET) substrates and investigation of their morphological, structural, optical and electrical properties are the main scopes of this thesis. In the first part of the study, CdS thin films were deposited on PET via electrodeposition method. Taking the advantages of electrodeposition methods, CdS thin films with good optical and electrical properties were produced. CdS thin films were also deposited on soda-lime glass substrates in order to observe substrate effect. Scanning electron

microscopy equipped with energy dispersive X-ray (SEM-EDX), X-ray diffraction (XRD) and UV-vis spectrometry have been used to determine the structural and optical properties of the films deposited at various temperatures and for different deposition time intervals.

For all samples, molecularly homogenous CdS films have been observed with atomic percent ratios of the Cd to S very close to 1:1. Thin films showed (002) hexagonal crystal structure around  $26^\circ$  ( $2\theta$ ) with average grain size 7.0 nm. CdS films have high transmittance for the wavelength greater than 500nm. Band gap energies of the films, which range between 2.74 and 2.68 eV, decreased with increasing both deposition temperature and time. For further characterization, photoelectrochemical performances and electrochemical impedance spectroscopy (EIS) of both as deposited and  $\text{CuCl}_2$  treated CdS thin films have been investigated. Later, following to the deposition of individual CdS thin films, polypyrrole thin films were produced and then heterojunctions of polypyrrole with CdS were examined. It has been observed that cadmium sulfide enhanced the photoelectrochemical properties of the polypyrrole film. Influence of the polypyrrole thin film deposition time on the photoelectrochemical properties has been also investigated in this study. Frequency dependent measurements revealed that type of charge carrier changes as a function of polypyrrole deposition time.

**Keywords:** Cadmium sulfide, Polypyrrole, Thin Film, Semiconductor, Photovoltaic, Morphological Properties, Optical Properties, Electrical Properties, Photoelectrochemical Properties.

# ÖZ

## BÜKÜLEBİLİR FOTOVOLTAİK UYGULAMALAR İÇİN YARIİLETKEN İNCE FİLMLEİN SENTEZİ VE KARAKTERİZASYONU

Tezel, Tamer

Yüksek Lisans, Kimya Bölümü

Tez Yöneticisi: Prof. Dr. Zuhâl Küçükyavuz

Yardımcı Tez Yöneticisi: Yrd. Doç. Dr. Nurdan Demirci Sankır

Eylül 2009, 70 sayfa

CdS ince filmleri fotovoltaik cihazlar dışında elektronik, biyo-etiketleme ve floresent görüntüleme alanlarındaki potansiyel uygulamaları ve ayarlanabilen optik özelliklerinden ötürü çok ilgi çeken malzemelerdir. Yakın zamanda, bükülebilir fotovoltaik cihazlar hafiflik, mekanik dayanıklılık ve geniş alanlarda uygulanabilirlikleri gibi özelliklerinden ötürü oldukça ilgi çekmiştir. Organik yarıiletkenler ve onların inorganik malzemelerle oluşturdukları heteroeklemler bükülebilir fotovoltaik cihaz uygulamaları için en çok gelecek vadeden malzemelerdendir.

Bu tezin başlıca amaçları; CdS ve Polipirol (PPy) ince filmlerinin bükülebilir polietilenterefitaleyt (PET) altlıkların üzerinde hazırlanması ve hazırlanan bu filmlerin morfolojik, yapısal, optik ve elektriksel özelliklerinin incelenmesidir. Çalışmanın ilk aşamasında, CdS ince filmleri elektriksel kaplama metoduyla PET

üzerine kaplanmıştır. Elektriksel kaplama metodunun avantajlarından yararlanılarak, iyi optik ve elektriksel özellikler gösteren CdS ince filmleri üretilmiştir. CdS ince filmleri, tutucu etkisini gözlemek için cam tutucular üzerine de üretilmiştir. Çeşitli sıcaklıklar ve kaplama sürelerinde üretilmiş ince filmlerin yapısal ve optik özelliklerinin belirlenmesinde EDX ekipmanlı Taramalı Elektron Mikroskopi (SEM-EDX), X-Işını Kırınım Cihazı (XRD) ve Ultraviyole ve Görünür Işık Absorpsiyon Spektroskopisi (UV-Vis) kullanılmıştır.

Tüm örnekler için, moleküler homojenlik gösteren CdS ince filmlerinde Cd ve S nin atomik yüzde oranının 1:1 e çok yakın olduğu gözlemlenmiştir. İnce filmler, ortalama 7.0 nm tane büyüklüğü ile  $26^\circ$  ( $2\theta$ ) civarında (002) altıgenel kristal yapısı göstermiştir. CdS ince filmleri 500 nm den büyük dalgalarda yüksek geçirgenlik göstermiştir. Filmlerin 2.74 ve 2.68 eV arasında değişen yasak enerji aralığı artan kaplama süresi ve sıcaklığına bağlı olarak azalma göstermiştir. İlave karakterizasyon için,  $\text{CuCl}_2$  işlemi görmüş ve görmemiş CdS ince filmlerinin fotoelektrokimyasal performansları ve elektrokimyasal empedans spektroskopisi incelenmiştir.

Daha sonra, CdS ince filmlerinin tek başına kaplanmasını takiben, PPy ince filmleri üretilmiş ve bu filmlerin CdS ile oluşturduğu heteroeklemler incelenmiştir. CdS nin PPy ince filmlerinin fotoelektrokimyasal özelliklerini arttırdığı gözlemlenmiştir. Bu çalışmada PPy ince filmlerinin kaplama zamanının fotoelektrokimyasal özellikleri üzerindeki etkileri de incelenmiştir. Frekansa bağlı ölçümler, yük taşıyıcının cinsinin PPy kaplama zamanının fonksiyonu olarak değiştiğini ortaya çıkarmıştır.

**Anahtar Kelimeler:** Kadmiyum sülfid, Polipirol, İnce Film, Yarıiletken, Fotovoltaik, Morfolojik Özellikler, Optik Özellikler, Elektriksel Özellikler, Fotoelektrokimyasal Özellikler.

**To my beloved family...**

## ACKNOWLEDGEMENTS

I wish to express my sincere appreciation and thanks to my supervisor Prof. Dr. Zuhâl Küçükyavuz for her guidance, valuable advices, moral support and for enlightening my professional and academic vision throughout my study.

I would like to express my sincere thanks to my co-supervisor Assoc. Prof. Dr. Nurdan Demirci Sankır for her endless support, guidance, patience and motivation throughout this work.

I wish to express my thanks to Prof. Dr. Mehmet Parlak and his staff from Department of Physics, Middle East Technical University for their technical support.

I would like to express my sincere thanks to Assoc. Prof. Dr. Mehmet Sankır for his valuable guidance, discussion and support.

I wish to express my special thanks to Bengi Aran, Yasin Kanbur and Dr. Serdar Atılğan for their endless help, unceasing encouragement and support.

I wish to thank to my dearest friend Bahadır Doğan for his valuable friendship, attitude and support throughout this work.

I would like to thank to my friends Berk Müjde, Can Nebigil, Alper Kılıklı, Oytun Ortaylı and Tuğba Özdemir for their precious friendship.

I wish to express my appreciation to the academic staff of METU Department of Chemistry for their professional support and guidance to the students of Department of Chemistry.

Finally, I would like to give the biggest thanks to my family who have made everything possible for me with their love, affection, support and guidance throughout my whole life. The completion of this study would not have been possible without them.

# TABLE OF CONTENT

ABSTRACT.....	iv
ÖZ.....	vi
ACKNOWLEDGEMENTS .....	ix
TABLE OF CONTENT .....	xi
LIST OF TABLES .....	xiii
LIST OF FIGURES.....	xiv
ABBREVIATIONS.....	xvi
CHAPTERS	
1. INTRODUCTION.....	1
1.1. SEMICONDUCTOR THEORY .....	1
1.1.1. THE BAND THEORY OF SOLIDS .....	2
1.1.2. TYPES OF SEMICONDUCTORS .....	5
1.2. SEMICONDUCTOR THIN FILMS .....	8
1.2.1. Applications .....	11
1.3. DEPOSITION METHODS FOR THIN FILMS .....	14
1.3.1. Selected Deposition Method: Electrodeposition .....	16
1.4. AIM OF THE WORK .....	18
2. EXPERIMENTAL .....	20
2.1. CdS THIN FILM DEPOSITION.....	20
2.2. POLYPYRROLE THIN FILM DEPOSITION.....	23
2.3. CdS/PPy HETEROJUNCTION .....	25
2.4. INSTRUMENTATION .....	25
2.4.1. Scanning Electron Microscope (SEM).....	25
2.4.2. Energy Dispersive X-Ray Spectroscopy (EDX) .....	25
2.4.3. X-Ray Diffraction (XRD) .....	25
2.4.4. UV-Vis Spectroscopy.....	26
2.4.5. Potentiostat .....	26

3. RESULTS AND DISCUSSION .....	27
3.1. CdS THIN FILMS .....	27
3.1.1. CdS Thin Film Deposited on Polyethylene Terephthalate (PET) .....	27
3.1.2. Photoelectrochemical and Electrochemical Impedance Performances of CdS Thin Films and the Effect of CuCl <sub>2</sub> Treatment on CdS Thin Films ....	33
3.1.3. CdS Thin Films Deposited on Soda Lime Glass Substrates .....	44
3.2. PPy and CdS/PPy THIN FILMS .....	51
4. CONCLUSIONS .....	61
REFERENCES .....	63

## LIST OF TABLES

### TABLES

Table 1 Effect of deposition temperatures and time on grain size .....	30
Table 2 Maximum optical transmittance and band gap energy data for the CuCl <sub>2</sub> treated CdS thin films deposited for different time.....	36
Table 3 Photoelectrochemical parameters of CdS thin films.....	37
Table 4 Band gap energies of CdS thin films deposited onto ITO coated soda-lime glass at 125°C.....	50
Table 5 Band gap energies of CdS thin films deposited onto ITO coated soda-lime glass at 125°C.....	50
Table 6 Photoelectrochemical parameters of Ppy and Ppy/CdS thin films.....	54

## LIST OF FIGURES

### FIGURES

Figure 1.1. Energy band gaps in materials .....	4
Figure 1.2. p-n junction .....	8
Figure 2.1. Gamry G750 Potentiostat/Galvanostat/ZRA system as a hardware integrated with a computer .....	26
Figure 3.1. SEM pictures and EDX analysis results of CdS thin films deposited onto ITO PET under 3V bias for 20 min at (a)-(d) 110 °C, (b)-(e) 100°C and (c)-(f) 90°C .....	28
Figure 3.2. X-ray diffraction pattern of CdS thin films growth on (a) ITO coated PET and, (b) ITO coated glass for various times .....	29
Figure 3.3. (a) Transmittance, (b) $(\alpha h\nu)^2$ versus photon energy $h\nu$ plot of CdS thin films deposited onto ITO coated PET at 100°C, under 3V bias for different deposition time. ....	32
Figure 3.4. (a) Transmittance versus wavelength and, (b) $(\alpha h\nu)^2$ versus photon energy $h\nu$ plot for the CuCl <sub>2</sub> treated CdS thin films growth for different time intervals .....	34
Figure 3.5 Photoelectrochemical cell configuration with three-electrode cell.....	35
Figure 3.6. Current density-Voltage characteristic of (a) as deposited, (b) CuCl <sub>2</sub> treated CdS thin films.....	38
Figure 3.7. The Mott–Schottky plot of (a) as deposited, (b) CuCl <sub>2</sub> treated CdS electrode in sulfate electrolyte under 35 mW/cm <sup>2</sup> illumination.....	40
Figure 3.8. Nyquist plots of (a)-(c) as-deposited CdS thin films, (d) CuCl <sub>2</sub> treated samples .....	42
Figure 3.9. Bode plots of (a) as-deposited and (b) CuCl <sub>2</sub> treated CdS thin films....	43
Figure 3.10. SEM pictures of CdS thin films deposited at 125 °C for (a) 60 min, (b) 30 min, (c) 20 min, and (d) 10 min on ITO coated soda lime glass substrates.....	44

Figure 3.11. Relationship between deposition time and Cd:S atomic ratio .....	45
Figure 3.12. X-ray diffraction patterns of CdS thin films deposited onto ITO coated glass substrate at 125 °C for a) 10 min b) 20 min, and c) 30 min.....	46
Figure 3.13. X-ray diffraction patterns of CdS thin films deposited onto ITO coated glass substrate at 125 °C for 10 min and annealed at a) 150, b) 250, and c) 350 °C.....	47
Figure 3.14. Relationship between grain size of the films and deposition time. ....	48
Figure 3.15. Transmittance versus wavelength plot of CdS thin films deposited onto ITO coated glass substrates at 125°C, for three different deposition time.....	49
Figure 3.16. SEM pictures of Ppy thin films grown on ITO-PET at room temperature for (a) 30 sec, (b) 1 min, (c) 5 min .....	52
Figure 3.17. UV-vis spectra of Ppy thin film grown for 1 min on ITO-PET.....	53
Figure 3.18. Current density-Voltage characteristic of (a) Ppy (b) Ppy/CdS thin films deposited on ITO-PET .....	55
Figure 3.19. The Mott–Schottky plot of Ppy and Ppy/CdS electrode.....	56
Figure 3.20. (a) Nyquist and (b) Bode plots of Ppy thin films.....	58
Figure 3.21. (a) Nyquist and (b)Bode plot of Ppy/CdS thin film.....	60

## ABBREVIATIONS

<b>Cd</b>	<b>Cadmium</b>
<b>S</b>	<b>Sulphur</b>
<b>CdS</b>	<b>Cadmium Sulfide</b>
<b>PET</b>	<b>Polyethylene Terephthalate</b>
<b>ITO</b>	<b>Indium Tin Oxide</b>
<b>PPy</b>	<b>Polypyrrole</b>
<b>CdTe</b>	<b>Cadmium Telluride</b>
<b>SEM</b>	<b>Scanning Electron Microscope</b>
<b>EDX</b>	<b>Energy Dispersive X-Ray</b>
<b>XRD</b>	<b>X-Ray Diffraction</b>
<b>PEC</b>	<b>Photoelectrochemical Cell</b>
<b>EIS</b>	<b>Electrochemical Impedance Spectroscopy</b>
<b>CdCl<sub>2</sub></b>	<b>Cadmium Chloride</b>
<b>CuCl<sub>2</sub></b>	<b>Copper Chloride</b>
<b>DMSO</b>	<b>Dimethyl Sulfoxide</b>
<b>Na<sub>2</sub>S</b>	<b>Sodium Sulfide</b>
<b>NaOH</b>	<b>Sodium Hydroxide</b>

# CHAPTER 1

## INTRODUCTION

### 1.1. SEMICONDUCTOR THEORY

Generally; semiconductor is defined as a solid-state material having an intermediate conductivity between a conductor and an insulator. Semiconductor devices have played an important role in the advance of modern electronics in the 21<sup>st</sup> century with the development of several electronic devices such as radios, telephones, transistors, computers and photovoltaics.

Today, several materials of the semiconductor family such as silicon, gallium arsenide, germanium, cadmium sulfide and cadmium telluride are being used in semiconductor industry. Starting with the first silicon integrated circuits produced in 1958 [1], semiconductor technology has evolved with a rapid pace up to date where high-tech microprocessors, solar cells and many other electronic devices are made of semiconductors. Electronic industry cannot survive if semiconductors and related technologies are neglected and that's why semiconductors proved to be the backbone of electronics. Although, today the semiconductor technology is mostly based on silicon, investigation and research in other materials and successive integration of new semiconducting materials with the potential technology may supersede the domination of silicon in the near future.

In the last decades, with the development of nanotechnology and polymer science, not only more efficient but also more cost effective semiconducting thin film materials have been produced. Nanomaterial thin films are being investigated to be used as n-type semiconductor material for the purpose of efficient solar absorption in solar cells. Also, new methods for preparing p-type semiconductors are being

developed to achieve the maximum light transmittance. Briefly, nanotechnology and polymer science and technology oriented semiconductor devices have carried the research progress in semiconductors to a new step where the improvement of chemical and physical properties of semiconductor materials is aimed.

In order to understand the nature of semiconductors, the difference between semiconductors, conductors and insulators must be fully understood. Moreover, some key concepts such as the band theory of solids, doping processes and p-n junction theory can give a general idea about the fundamentals of semiconductors.

### **1.1.1. THE BAND THEORY OF SOLIDS**

It is important to understand the band theory of solids, since this theory describes the nature of semiconductors in terms of the energy levels between valence and conduction bands. The main difference between a semiconductor and a metallic conductor is that, in metallic conductors the current is carried by the flow of electrons whereas in semiconductors, this work is done by not only the flow of electrons but also the flow of positively charged holes. These positively charged holes occurs in the absence of electrons in the bonds where they act as positive charge carriers.

Electrical conductivity, which is in the heart of semiconductor theory, is highly related to the band structure of a material. When two unique atoms are separate enough from each other, the atomic energy levels of each single atoms are equal. When these atoms come closer, an interaction is born between these atoms resulting in differences in their original energy levels and consequently forming molecular bands. Materials with different type of conductivity exhibit different band structures. In conductors, the energy difference between partially filled energy levels and the unoccupied states is very low. When a potential is applied to a metal, electrons are accelerated and they can easily flow through the unoccupied states since very low energy is needed to boost this motion between the occupied and

unoccupied states. Hence, it is almost impossible to talk about a particular set called *valence band* and *conduction band*.

As mentioned before, there must be an empty energy level for an electron to move, otherwise, in the absence of an empty state, electrons cannot move in a solid. This means, if a band is fully occupied with electrons, no movement will take place although a potential is applied. Therefore, no current will be observed if there is no electron passing from an occupied state to an unoccupied one. With respect to this phenomenon, it can be clearly understood why there is no current observed in insulators. In insulators, valence band is the highest band fully occupied (HOMO) by electrons and the conduction band is the lowest unoccupied band (LUMO) and there is a *forbidden band gap* between these two bands equal to a value between 5 to 10 eV [2]. This large band gap value between the valence band and the conduction band prevents electrons to reach the conduction band and as a result no current flows in insulator materials.

Similar with the band structure of insulators, semiconductors possess a valence band occupied by electrons and a conduction band ready to be filled with electrons. There is also a band gap between these two allowed bands like the one in an insulator. The main difference between the band gap in insulators and the band gap in semiconductors that, the value of the band gap is much smaller (1.1 eV for silicon) [3] in semiconductors compared to the one in insulators. This means more electrons are found in the conduction band in semiconductors. Since in semiconductors thermal energy is the driving factor of exciting electrons, the conductivity of semiconductors depends on the temperature. The conductivity of a semiconductor material as a result of a decrease in resistivity is caused by frequent collisions with increasing kinetic energy, increases with increasing the temperature. Figure 1.1 summarizes the energy band gaps in conductors, semiconductors and insulators.

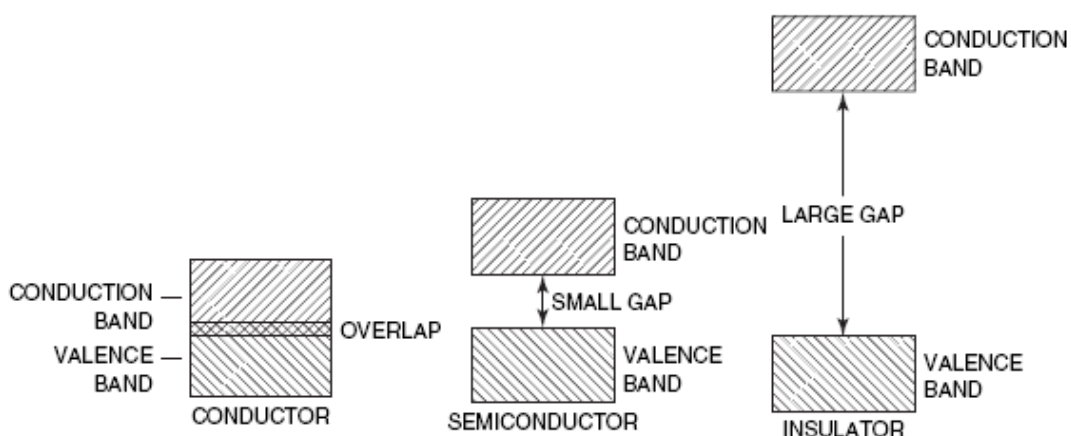


**Figure 1.1.** Energy band gaps in materials

Movement of electrons between valence band and conduction band describes the basic process of the flow of current in semiconductors. In semiconductors the valence band, which is below the forbidden band gap, is almost completely occupied and above the forbidden band gap there is the conduction band which is almost empty. Being almost full of electrons in the valence band and possessing immobile electrons, flow of current does not take place in semiconductors unless the electrons are excited by a source of energy. When a semiconductor material absorbs a photon and if the energy of the photon is greater than the forbidden band gap, electrons can be excited to the conduction band where they can flow easily. As a result of the movement of an electron from valence band to conduction band leaves a hole in the place of the excited electron which can flow through the material and acts as a positively charged particle. Two important processes – *carrier generation* and *recombination* [4] are the key factors for the creation of charge carrying electrons and positively charged holes.

Specifically for the organic semiconductors, one important property is the continuous series of the double bonds which brings in the conjugated character of the structure. Normally, almost all organic solids are insulators. A large energy band gap exists between the occupied bonding orbitals and unoccupied antibonding

orbitals and this band gap's value is beyond the visible range of the spectrum. Therefore, the band gap between the highest occupied molecular orbital (HOMO) and the lowest unoccupied molecular bonding orbital (LUMO) is large in long chains of bound carbon atoms. This is the reason for the insulating behaviour. However in conjugate organic polymers, because of the  $sp^2$  hybridisation character of carbon atoms,  $p_z$  orbitals that are perpendicular to  $sp^2$  orbitals form additional  $\pi$ -bonds. These  $\pi$ -bonds have less energy difference compared to the energy difference between HOMO and LUMO states. Consequently, this brings in semiconductor properties such as strong absorption in the visible region of the spectrum. In order to make an analogy for the electronic structure of organic semiconductor with the electronic structure of inorganic semiconductors, one can say that in organic semiconductors HOMO state becomes valence band, LUMO state becomes conduction band, carbocations become positively charged holes and carbanions become electrons[5].

### **1.1.2. TYPES OF SEMICONDUCTORS**

In general, semiconductors, depending on doping level, can be classified under two main groups:

- Intrinsic Semiconductors
- Extrinsic Semiconductors

Intrinsic semiconductors are pure semiconductors which means they are not doped by any impurities. In this type of semiconductor, conductivity comes from thermal excitation of electrons. In intrinsic semiconductors, as a result of charge carrier and recombination steps, the number of excited electrons and positively charged holes are equal [6].

In order to enhance the conductivity of intrinsic semiconductors due to their low conductivity and inconvenience for many applications, an important process called *doping* is applied to semiconductors. In this type of process conductivity of a semiconductor is changed by altering the concentrations of charge carrier electrons and positively charged holes with addition of impurities in small amounts.

By adding impurities into the crystal structure of the original material, the aim is to change the electronic structure, however, crystal structure remains same. For instance, addition of an atom, Arsenic, having five valence electrons to an atom, Germanium, having four valence electrons will cause Arsenic atom enter into the covalent bond with Germanium atom. The extra fifth electron of Arsenic atom is free to move from one atom to another hence making it available for conduction. Addition of an Arsenic atom into the crystal structure of Germanium atoms causes an impurity and this impurity is called *donor impurity* [7]. This type of semiconductor, where the impurity donates an electron, is called *n-type semiconductor*. Besides the fact that free electrons are produced in n-type doping, equal number of positive charges are also produced in pairs with the free electrons. Therefore, the semiconductor material that is doped with an impurity remains electrically neutral. However, this positive charges should not be understood as positively charged holes. These charges occur in the absence of the free electron and do not contribute to a current flow. One major important advantage of the free electron's contribution to the pure semiconductor is that the donor electron is much more closer to the conduction band than an electron in the valence band of the original atom. The donor electron exists in another energy level which is much narrower than the energy level for the valence electrons and making the flow of current easier in the n-type semiconductor.

On the other hand, if a pure semiconductor - say Germanium again- is substituted with - Gallium - having three valence electrons, this type of semiconductor is called *p-type* [8], since three of the four covalent bonds are occupied, the fourth bond remains empty and acts as a hole that relatively moves in the opposite direction of a

moving electron. Actually this is not a real motion, in fact this is a relative motion caused by the motion of electrons from one bond to another and leaving a hole behind after their move. Similar with the energy band structure of n-type semiconductors that is different than the pure semiconductor, p-type semiconductors also differs in the band structure from pure semiconductors by having an acceptor energy level higher than the valence band and attracting electrons to start a current flow.

Similar to the inorganic semiconductors, organic semiconductors can be n- or p-type, depending on the type of the charge carrier radicals in the polymer backbone. The charge transport mechanism of the organic semiconductors are based on the motion of these radicals, which are created by oxidation or reduction, along a polymer chain. PEDOT/PSS, polyaniline and polypyrrole can be listed as examples of p-type organic semiconductors. Tetra carboxylic dianhydride (NTCDA), carbon nanotubes are among the n-type organic semiconductors

*p-n junction* is an important concept in semiconductor theory. Simply, a p-n junction is achieved when a connection is established between a p-type semiconductor and an n-type semiconductor. p-n junction, also called heterojunction, are in great use for producing solar cells where a p-type semiconductor acts an absorber layer and a n-type semiconductor acts as a window layer.

One of the major characteristics of p-n junction is the depletion layer [9]. Depletion layer is a non-conducting layer formed when charge carrier electrons from n-type material and the positively charged holes from p-type material are interacted and eliminated. To describe in details, electrons of the n-type material diffuse to the p-region through the junction point and leaves holes behind in the n-region. At the same time, holes diffuse to n-region leaving the region near the junction point with negative charge. As a result, the region near the junction point becomes charged and

forms the depletion layer. Diffusion of the opposing charges stops when the Fermi energies of two materials coincide (Figure 1.2.).

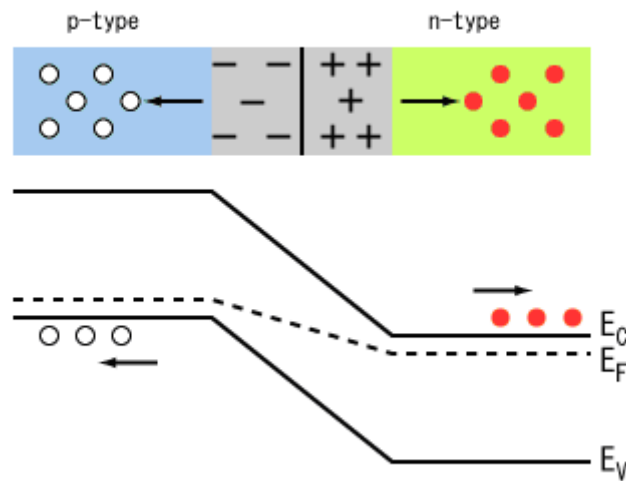


**Figure 1.2.** p-n junction

## 1.2. SEMICONDUCTOR THIN FILMS

Semiconductor thin films are made by depositing one or more thin layers and used in many applications such as transistors, sensors and photovoltaic devices. Structural, chemical and physical properties of semiconductor thin films are highly dependent on the deposition technique and they vary in thickness from a few nanometers to hundreds of micrometers. Thin films are formed by *random nucleation* and *growth* processes [10] which brings in many interesting properties. Today many of the semiconductor thin films that are used in photovoltaic industry are inorganic, however, new and functional organic semiconductor thin films have been produced for new technologies.

Many interesting properties of semiconductor thin films make them a promising and an ideal candidate for several applications. First of all, a large variety of chemical, electrochemical and physical deposition techniques enables a low cost fabrication of the semiconductor material over large areas in desired geometry and structure. Moreover, microstructures of the thin films such as amorphous, single crystalline, polycrystalline and nanocrystalline structures can be obtained by changing deposition technique, temperature or substrate. Different types of junctions between different semiconductor materials can be acquired in order to improve electrical property of the thin films.

Based on the properties of the semiconductor thin film material, different type of solar cells have been produced up to date. Most commonly used thin film semiconductors among the others are inorganic thin films. These inorganic thin films can be either homojunction, where two similar semiconductor material forms a junction layer, such as n-type silicon and p-type silicon, or heterojunction, where two different semiconductor material forms a junction layer, like n-type cadmium sulfide (CdS) and p-type cadmium telluride (CdTe).

Silicon thin films are the most popular type of inorganic semiconductor material and have been widely used in electronics and photovoltaics since the beginning of semiconductor thin film industry. Being an ideal solar cell material, silicon thin films have been produced in amorphous, polycrystalline and nanocrystalline forms with reported deposition techniques such as chemical vapor deposition (CVD) [11]. Remarkable progress is taking place in improvement and integration of polycrystalline silicon thin films, where cell efficiency of 15% has been reported [12]. Amorphous silicon (a-Si:H) thin film solar cells are being produced since the mid 1970's [13] however, because of stability and low efficiency problems a-Si:H thin films have limited use compared to crystalline silicon thin films. Silicon thin films are usually deposited on stainless steel and ceramic substrates.

Besides silicon semiconductor thin films, copper indium selenide ( $\text{CuInSe}_2$ ) thin films are being used in photovoltaic cells.  $\text{CuInSe}_2$  has a band gap value of around

1.0 eV and cell efficiencies over 19% with CuInSe<sub>2</sub> solar cells have been reported [14].

CdS semiconducting thin films proved to possess high potential for photovoltaic applications and this type of thin film will be analyzed more detailed in the experimental part.

Considering organic semiconductors as a relatively new technology, these materials offer many exciting opportunities in optoelectronics with having several advantages such as flexibility, lower technology processing and therefore, lower manufacturing cost[15]. Improved electronic properties of organic semiconductors have lead these materials to be used for microelectronic and optoelectronic devices such as, photovoltaics [16], light emitting diodes [17], field effect transistors [18] and integrated circuits [19]. Organic semiconductors can be divided into two major groups as molecular and polymeric semiconductors [20].

On the other hand, polymer organic semiconductor materials derived from polyacetylene, polypyrrole and polyaniline [21] consist of linked chains of monomers and possess conjugated bonds and achieve conductivity. Since, many of the polymers are more soluble than small organic molecules in common solvents, deposition methods such as spin coating is preferred where small organic molecules are deposited by vacuum evaporation. Polymer organic semiconductors have an advantage of combining the properties of several monomers and they display the better mechanical properties. Moreover, polymer organic semiconductors give the better results in deposition such as homogenous and pinhole free surfaces compared to the morphological properties of small molecular organic semiconductors.

Polypyrrole (PPy) is known as one of the most stable conducting polymers to be used in semiconductor and electronic applications. Polypyrrole is a heterocyclic compound formed from a number of pyrrole rings, consisting of carbon and nitrogen. Pyrrole is able to polymerize electrochemically to form PPy. PPy is an important member of the conducting polymer family and has been investigated

extensively for the preparation conditions on its properties since it was first electrochemically synthesized by Diaz et al. [22]. PPy thin films are intrinsically conducting polymers and have a wide field of application where they are used as electrochromic devices, capacitors, anticorrosive coatings, batteries and sensors [23,24].

### **1.2.1. Applications**

Semiconductor materials have been used in electronic industry for more than 50 years in order to manufacture a large variety of devices including, diodes, transistors, sensors, microprocessors and solar cells. Semiconductor thin films have also been used widely in the applications developed in semiconductor technology, however the most common area that benefits semiconductor thin film technology is the photovoltaic devices.

Simply, photovoltaics is the field of technology that is related to the usage of solar energy to produce solar cells. The importance of photovoltaics comes from the fact that photovoltaics are not only important in terrestrial applications to gain renewable and clean energy, but also enables the benefits of solar energy which can be used as a major source of electrical power for space systems [25]. Besides, concerns over the global climate change has driven the attentions to use environmentally friendly energy sources instead of the conventional ones, where photovoltaics seem to be the new trend. The most obvious proof for this trend is the annual increase rate of the production of photovoltaics which is 35 % per year, from 88.6 MW in 1996 to 744.8 MW in 2003 [26]. By 2005, Germany had the record with an installed potential of photovoltaic power with 1229 MW covering 83.79 % of the production in Europe, where Turkey had only total installed capacity of 0.5 MW [27].

Today, crystalline silicon products have dominated over 90 % of the production of solar cells [28]. The rest is composed of thin film solar cells produced from

amorphous silicon, CdTe and CIGS materials. Over the last decade the production of CdTe and CIGS solar cells have increased due to the promising efficiencies obtained from these technologies. At the moment, crystalline silicon holds the record with an efficiency of 24 % where the maximum efficiency of a thin film solar cell, a CIGS solar cell, reported so far is 19 %. Besides, an efficiency of 16.5 % for CdTe and 12.4 % for a-Si:H has been achieved [29].

Thin film solar cells are composed of several thin layers of different material deposited on various substrates. The common structure of the solar cell consists of a substrate, either rigid or flexible, a transparent conducting oxide (TCO), a window layer made of n-type semiconductor, an absorber layer made of a p-type semiconductor and a metal contact. Each of these components have different physical and chemical features and the overall performance of a solar cell depends on the properties of the components and the compatibility between them.

Substrate is the backbone of the whole device that the layers are deposited on. Main role of the substrate is to provide a mechanical strength for the device. Substrates are generally transparent to allow the incoming light to penetrate into the solar cell and the contact between the window layer and the substrate is made by a conducting oxide coated on the substrate. Non-transparent substrates are metallic or metal coated glass/polymer which does not need a contact since it acts as a contact itself. Substrates must be mechanically stable and in match with the properties of the deposited layers. High deposition temperature during fabrication requires rigid substrates such as glass, since flexible substrates are not stable at high temperatures. It is also reported that substrates have direct effect on the efficiency of the cells and the grain quality of the grown films [30-32].

Transparent conducting oxides (TCO) provides a contact between the substrate and the window layer with good electrical conductivity and high transparency in the visible region. Good conductivity is needed to reduce the series resistance of the

device and high transparency is needed to ensure that the incident light transmitted to the absorber layer.

Window layer, in heterojunction with an absorber layer, has a function of directing the maximum amount of incident light to the junction point and absorber layer. Lattice matching of the window layer with the absorber layer is important for the device performance. In most of CIGS solar cells CdS is used as a window layer and for CdTe solar cells, CdS still remains the best heterojunction partner [33-36].

Absorber layer is an efficient absorber and used as the p side of the p-n junction. Heterojunction solar cells are named with respect to the material used as the absorber layer. For instance, if the absorber layer is CIGS then the cell is named as CIGS solar cell. CIGS is a desirable absorber material with a band gap of 1.53 eV. CdTe is another absorber material with having a band gap around 1.5 eV. A-si:H, polycrystalline silicon and some organic semiconductors such as dyes, pigments and polymers [37] are also used as absorber layers in solar cells.

The back contact is composed of a metal layer that provides a low resistance electrical connection to the absorber layer. Gold (Au) is mainly used in CdTe solar cells. Also, molybdenum (Mo) is used for CIGS solar cells [38] and promising results are obtained from nickel (Ni) based back contacts [39].

Photoelectrochemical cell (PEC) is another type of solar cell that generates electrical energy from light. The main difference between a photovoltaic cell and a PEC is the electrolyte solution that the cell is immersed in. A PEC is made up of a semiconductor photoactive n- or p-type working electrode and a counter electrode which are both immersed in an electrolyte solution. PECs are mainly used as an electrochemical photovoltaic cell and for the photogeneration of hydrogen which can be used as fuel.

### 1.3. DEPOSITION METHODS FOR THIN FILMS

Deposition process is the major key for producing devices such as microelectronic devices, computers, solar cells which are based on thin film technology. Progress in improving the device performance has demanded suitable thin films with high quality, requiring fast, cheap and effective deposition methods. The best intentions in improving deposition techniques for thin films have provided the researchers a better understanding in the physical and chemical nature of the films, connection layers, surface properties and microstructures. Semiconductor industry which is almost totally based on solid thin films have revealed the importance of deposition technology and helped it to evolve rapidly in the last decades.

There are several methods for creating thin films in the thickness range of nanometers to micrometers. Basically deposition methods can be classified into two groups: Physical and chemical deposition [40].

(i) Chemical deposition methods

- Chemical Vapor Deposition
- Chemical Bath Deposition
- Electrodeposition
- Molecular Beam Epitaxy
- Thermal oxidation

(ii) Physical Deposition methods

- Physical Vapor Deposition ( Evaporation and Sputtering )

*Chemical Vapor Deposition* (CVD) is used for creating high purity and effective solid thin films [41,42]. In this process the substrate is placed inside a reactor where it is exposed to volatile gases and as a result of chemical reactions between the

source gases and the substrate, a solid product is formed on the surface of the substrate. By this technique, single crystalline, polycrystalline and amorphous thin films can be produced with high purity.

The major feature of CVD is its processibility for synthesizing both single and complex materials with the desired purity at low temperatures. The chemical and physical properties of the materials to be deposited can be determined by controlling the reaction and deposition conditions such as temperature, pressure, gas flow rate and gas concentration. Chemical reaction types that take place in the reactor are oxidation, reduction, pyrolysis, hydrolysis and compound formation.

*Molecular Beam Epitaxy* (MBE) [43,44] is a method for creating single crystal thin films. It is a complicated method that takes place under high vacuum. Slow evaporation of the constituents of the film results in the formation of thin films on the substrates. Ultra pure elements, such as gallium and arsenic, are produced and heated at furnaces, then slowly sublimate and finally by reacting with each other they condense on the substrate to form pure compounds. In the case of producing organic semiconductors by MBE, the molecules are condensed on the substrates instead of elements. The major advantage of MBE is its process temperature which is suitable for producing several single crystalline thin films.

*Chemical Bath Deposition* (CBD) is a technique in which the substrate is kept in a solution containing metal and sulphur ions at a constant temperature. The first semiconductor thin films produced by CBD were PbS and PbSe photodetectors [45]. Later CdS and CdSe thin films started to be produced by CBD and it became an important process in solar cell production. This technique, by time, proved to be an ideal method for the production of large area thin films containing highly insoluble products.

*Thermal oxidation* [46,47] is another method in which chemical processes take place in gas phase as in CVD. In thermal oxidation, substrate which is the source of semiconductor constituent is oxidized in oxygen rich environment. Compared with

CVD, this method is more limited since substrate is consumed in deposition; however thermal oxidation provides high purity and quality of oxide films for the semiconductor industry. Another limitation shows itself in film thickness since the film growth is formed by the diffusion of oxygen into the substrate and naturally by time, diffusion of oxygen becomes more difficult and limits the film thickness. Furthermore, only some materials which can be oxidized are used and only oxide thin films of the substrate can be produced by this method.

*Physical Vapor Deposition (PVD)* is a general term for the methods that work with the production of thin films in which condensation of vaporized materials released from a source is transferred into substrates. PVD methods that are related to the production of thin films are *sputtering* and *evaporation*.

*Sputtering* is an etching method in which surface atoms from a target source are ejected and deposited on the substrate. In sputtering, the vapor of the target source, ejected surface atoms, fly in straight lines and make an impact on the surface of the substrate resulting in the formation of a thin film. Sputtering method has some major advantages such as, the evaporation of highest melting point materials, achieving desired composition close to the composition of the source material and a better adhesion of thin films over the surface compared to the evaporated thin films.

*Evaporation* is another common PVD method for depositing thin films. In evaporation, the source material is evaporated in a vacuum tube where the evaporated particles are condensed over the substrate to form a solid thin film. The major advantage of evaporation over sputtering is its fast processibility.

### **1.3.1. Selected Deposition Method: Electrodeposition**

As mentioned before, thin films can be obtained by various methods by either chemical or physical methods. Most of these methods provide low cost solutions. However, full potential of these methods for obtaining maximum quality films have

not been clarified yet. On the other hand, electrodeposition which is the most simplest, the most known and one of the cheapest of the chemical methods resulted in efforts to produce high quality semiconductor thin films recently.

Previous success achieved in depositing metal and metal alloys electrochemically has attracted attention to improve the electrodeposition process for producing large area, cost effective and low temperature processing semiconductor thin films. The advantageous features, such as the ability to produce uniform films over large areas, low temperature solutions for the substrates that are unstable at high temperatures and the possibility to achieve the desired properties of the films by controlling the deposition conditions in a contemporary computer controlled system, that electrodeposition method displays has provided a wide range of industrial experience in electrodeposition.

In the simplest way, electrodeposition system consists of an electrolyte solution containing metal ions as well as other ions to maintain the flow of electricity, a substrate as a working electrode, a reference electrode and a counter electrode. Due to the electric field, current flow inside the electrolyte results in the movement of cations and anions towards the cathode and anode and eventually depositing on the substrate as a result of charge transfer reaction. One important factor in electrodeposition of the thin films is the properties of the substrate. First of all the substrate must be conductive, otherwise no deposition will occur on the surface of the substrate. That is why non-conductor substrates are coated by a conducting material layer. Secondly, substrates must be clean and the surface should be smooth. Unclean surface of the substrate will result in inhomogenities over the surface. Finally, substrates should have mechanical strength and should be stable in electrolytic solution.

Different electrodeposition methods are present for the elemental semiconductors, such as silicon and germanium, as well as for compound semiconductors. Electrodeposition, as a chosen method for thesis work, of CdS and PPy thin films

are performed in this study. Non-aqueous and aqueous electrodeposition conditions and the chemical reactions that take place during electrodeposition of these thin films will be extensively discussed in the experimental part.

#### **1.4. AIM OF THE WORK**

In this study, synthesis of CdS, polypyrrole thin films and to produce the heterojunctions of CdS/PPy thin films on flexible PET substrates was aimed. Thin films were deposited electrochemically since electrodeposition is a well known, low cost technique which is suitable for low temperature laboratory scale production of thin films. Several characterization methods were used in order to investigate the chemical, physical and electrical properties of the deposited films.

The reason for studying CdS thin films is the fact that, CdS is a promising candidate for the new generation photovoltaic devices. Being made by straight-forward and low cost deposition techniques, CdS have proved to form homogenous and high quality thin films. Although several studies have been reported about this subject, still many research groups are working on enhancing the properties of CdS thin films. Therefore, one of the objectives of the thesis work is to synthesize CdS thin films that would be a perfect match with the flexible photovoltaic applications.

Synthesis of polypyrrole thin films is aimed in order to investigate polymer semiconductor properties. Heterojunction of CdS/PPy was performed to observe the junction properties of an inorganic and a polymer thin film.

The thin films were deposited on PET substrates, which are cheap, commercially available and lightweight flexible substrates. Glass substrate is also used in some part of the work in order to compare the properties of the CdS thin films deposited on different type of substrates.

Morphological properties and chemical compositions of the thin films were observed by Scanning Electron Microscope (SEM) and Energy Dispersive X-Ray Analysis (EDAX) respectively, crystal structure and grain sizes of the films were determined by X-Ray Diffraction (XRD), transmittance, absorption and band gap values were calculated by UV-Vis Spectroscopy, photoelectrochemical properties were investigated by PEC method and electrochemical impedance spectroscopy results were obtained by Potentiostat/Galvanostat/ZRA system.

## **CHAPTER 2**

### **EXPERIMENTAL**

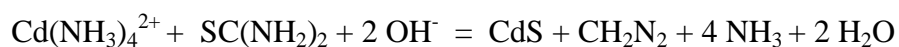
#### **2.1. CdS THIN FILM DEPOSITION**

CdS has been one of the most widely used semiconductor thin film material for photovoltaic applications, optical detectors and optoelectronic devices [48]. CdS is an II-IV group semiconductor compound with having an energy band gap of 2.42 eV. CdS is a desirable semiconductor material and it is used as a window layer in the solar cell. The major reason that makes CdS thin film so attractive for this purpose is that CdS is transparent in the visible part of solar spectrum which enables sun light to penetrate into the absorber layer therefore giving a rise to photovoltaic effect. CdS thin film provides the n-part of a p-n heterojunction solar cell system.

Deposition technique plays an important role in establishing a good p-n junction since the properties of the junction depends on the quality of the interaction of the n-type and p-type semiconducting material. The most suitable techniques for producing CdS thin films with good junction properties include sputtering [49], close spaced sublimation (CSS) [50], high-vacuum thermal evaporation (HVTE) [51,52], molecular beam epitaxy (MBE) [53], chemical bath deposition (CBD) [54-57] and electrodeposition [58].

CdS thin films can be deposited on large variety of substrates such as metal foils, glass and flexible polymers like the other metal chalcogenides. In CBD, this is done by dipping the substrates into a solution containing metal complex and sulfide ions. CBD displays an example of a low cost technique for preparing high quality CdS films to be used in CdS/CdTe heterojunction solar cells. Basically, in CBD, CdS

films are prepared in a solution of cadmium salt where decomposition of thiourea takes place.



A reaction of CBD of CdS can contain an aqueous solution of cadmium acetate ( $\text{Cd}(\text{CH}_3\text{CO}_2)_2$ ) as a cadmium ion source, thiourea ( $\text{N}_2\text{H}_4\text{CS}$ ) as a sulfur ion source, ammonium as a complexing agent and ammonium acetate ( $\text{CH}_3\text{CO}_2\text{NH}_4$ ) as a stabilizing buffer agent.

One important factor in CBD is the possibility of CdS to exist in its two crystalline forms, the hexagonal (wurtzite) and the cubic (zinc blende) [59-61], with adjusting the chemical composition of the bath, pH and temperature of the solution. By annealing the samples at 400 °C as a post treatment, it is possible to increase the ratio of hexagonal structured grains. A proof of this recrystallization is the energy band gap value of 2.42 eV that hexagonal structured CdS displays since the cubic structured CdS monitors lower band gap values. Annealing as a post treatment provides many benefits such as reorganization in the crystal structure and reevaporation of excess sulphur from the surface.

Close spaced sublimation (CSS) is another method for preparing semiconducting CdS thin films. In this method CdS is sublimed from a solid source where CdS source dissociates into its elements. The dissociated elements combine on the surface of the substrate and deposit a CdS layer. Rate of sublimation depends on the temperature and the pressure inside the reaction container so as the rate of CdS deposition. To obtain an inert atmosphere, argon gas is used however argon increases the pin holes on the surface of the thin film. Instead of argon, oxygen may be used to acquire pin hole free surface however deposition rate decreases in the presence of oxygen.

High performance CdS thin films can also be produced by evaporation of CdS layers and sputtering and electrodeposition, which will be discussed more detailed later. All of the methods mentioned above have particular properties to satisfy the

needs of the desired purpose. Since the optical and electrical properties of CdS thin films highly depends on the deposition technique, properties of the thin films have to be matched with the characteristics of the absorber layer that will be in contact with CdS layer. In a general aspect, sputtering, HVTE and MBE require specific tools, and therefore, their manufacturing cost is high. Moreover, they are limited by the sample size. Although CBD can be applied on large area substrates and is cost effective, it fails to application on flexible substrates [62].

### **2.1.1. Electrodeposition of CdS Thin Films**

Electrodeposition of CdS thin films were performed at + 3.0 V dc in an electrolyte solution containing 0.055 M CdCl<sub>2</sub>, 0.19 M elemental sulphur and 150 ml DMSO as a solvent [63]. Nitrogen gas flow was maintained, starting 10 minutes before deposition and during deposition in order to prevent CdSO<sub>4</sub> formation. After deposition, samples were washed with DMSO to remove excess sulphur from surface. CdS thin films were deposited on both ITO coated soda-lime glass and PET substrates, purchased from Sheldahl, USA, in order to observe substrate effect on the films. For CdS thin films deposited on glass substrates, depositions at four different deposition time, as 10, 20, 30 and 60 minutes, at 125 °C were performed. For the films deposited on flexible PET substrates, depositions were performed at several temperatures varying from 90 to 110 °C . Pt cage was used as a counter electrode, ITO coated glass and PET substrates were used as working electrodes and all the depositions were performed with a potentiostat. Annealing of the as-deposited films on glass substrates were carried out at 150, 250 and 350 °C for 30 minutes under nitrogen environment.

## 2.2. POLYPYRROLE THIN FILM DEPOSITION

Recently, there is a great interest in flexible photovoltaic devices due to their unique properties, such as, very low weight, mechanical durability and large area applications [64, 65]. Organic semiconductors and their composites with inorganic materials are the most promising candidates for this application. Several studies have been reported on flexible photoelectrochemical cells based on intrinsically conductive polymers such as polyaniline, polythiophene and polypyrrole [66, 67]. The main drawback of these devices is their low efficiency compared to crystalline and amorphous inorganic semiconductor based cells. Efforts have been made to increase the efficiencies of the “all-plastic” photoelectrochemical cells typically around  $10^{-2}$  - $10^{-1}$ % [68]. On the other hand, possibility of controlling the electrical and optical properties, environmental stability, low production cost, processibility and possibility of large area coating made these materials very attractive.

Polypyrrole (PPy), one of the most important conducting polymers, has been used widely in chemical sensor, corrosion protection and rechargeable battery applications [69-71]. Recently, there are number of studies on PPy thin films integrated into photoelectrochemical cell [72, 73]. Basically, like all conducting polymers, PPy produces free electrons and holes under illumination generating the photocurrent. High density of traps in the film, caused by a large number of defects, generates low mobility and therefore low efficiency. Combining the PPy with high performance materials including nano particles and other conducting polymers results the differentiated structure and electronic properties resulting the more efficient light harvesting [74].

In this study, polypyrrole and polypyrrole/cadmium sulfide (PPy/CdS) thin films have been electrochemically deposited on indium tin oxide coated polyethylene terephthalate (ITO-PET). Although, there have been some studies on electrochemical deposition of PPy on ITO-PET [75], according to our best

knowledge, this is the first time photoelectrochemical investigation of the PPy/CdS growth on ITO-PET substrate.

### **2.2.1. Electrodeposition of PPy Thin Films**

Pyrrrole monomer obtained from Aldrich was used after distillation and stored in a refrigerator. PPy thin films were grown at room temperature on ITO-PET substrate by potentiostatically controlled polymerization of pyrrole monomer using a Gamry G750 Potentiostat/Galvanostat/ZRA system. In order to determine the oxidation potential cyclic voltammetry was carried out in a three electrode cell containing aqueous solution of 0.02M pyrrole and 1 M H<sub>2</sub>SO<sub>4</sub> mixture. A platinum wire and a coil were used as working and counter electrode respectively. Also, a silver wire was used as reference electrode. The oxidation potential of the PPy was obtained around 1.0 V, which is in an agreement with previous studies [76, 77]. PPy thin films were potentiostatically deposited on ITO-PET using the same experimental conditions with cyclic voltammetry. CdS deposition has been carried out at 3.0 V, 100 °C for 30 min.

Morphological characterization of the thin films was performed using a QUANTA 400F Field Emission Scanning Electron Microscope. The absorbance spectra of the samples were measured by a Pharmacia LKB Ultraspec III UV-VIS spectrophotometer over the wavelength range of 325-900 nm at room temperature. Photoelectrochemical (PEC) cell configuration was formed with PPy or PPy/CdS thin film as working electrode into a three-electrode one compartment cell, with a graphite counter electrode and Ag/AgCl reference electrode. Electrical response of the thin films under illumination (35 mW/cm<sup>2</sup>) was recorded using a Gamry G750 Potentiostat/Galvanostat/ZRA system. 0.1 M Na<sub>2</sub>S, 0.1 M NaOH and 0.1 M S solution was used as electrolyte. For electrochemical impedance measurement same experimental conditions and setup was used.

## **2.3. CdS/PPy HETEROJUNCTION**

Previously obtained PPy thin films on flexible PET substrates were coated by a thin layer of CdS with the same procedure used for the electrodeposition of CdS thin films. PPy thin films deposited on PET substrates were used as the working electrode and Pt cage was used a counter electrode. CdS thin film deposition was carried out at 100 °C for 30 minutes.

## **2.4. INSTRUMENTATION**

### **2.4.1. Scanning Electron Microscope (SEM)**

SEM was used in order to collect images from the samples' surface for morphological studies. Samples were divided into small pieces with around 1 cm<sup>2</sup> surface area. Sample surfaces were coated with an ultrathin layer of gold/palladium alloy in order to enhance the electrical conductivity and improve resolution. Analysis was carried out by QUANTA 400F Field Emission Scanning Electron Microscope with 1.2 nm resolution in METU Central Laboratory.

### **2.4.2. Energy Dispersive X-Ray Spectroscopy (EDX)**

Chemical characterization and elemental analysis of the films were obtained from EDX which is connected to the QUANTA 400F Field Emission Scanning Electron Microscope.

### **2.4.3. X-Ray Diffraction (XRD)**

Crystal structures and grain sizes of the films were determined by Rigaku Miniflex X-ray diffraction system equipped with Cu K $\alpha$  radiation.

#### 2.4.4. UV-Vis Spectroscopy

The transmission spectra of the samples were measured by a Pharmacia LKB Ultraspec III UV-VIS spectrophotometer over the wavelength range of 325-900 nm at room temperature.

#### 2.4.5. Potentiostat

Electrodeposition of CdS and PPy thin films, EIS and PEC characterizations were carried out with a Gamry G750 Potentiostat/Galvanostat/ZRA system placed into a computer with a hardware operator. Potentiostat's main duty in this work is to maintain the working electrode at a specific potential with respect to the reference electrode during electrodeposition. Saturated Calomel Electrode (SCE) and Silver/Silver Chloride (Ag/AgCl) electrodes are the most used type of reference electrodes. Graphite and silver foil are used as counter electrodes during electrodeposition.

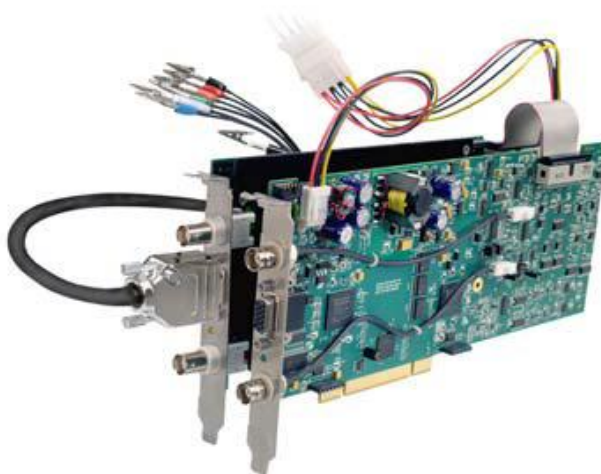


**Figure 2.1.** Gamry G750 Potentiostat/Galvanostat/ZRA system as a hardware integrated with a computer

## CHAPTER 3

### RESULTS AND DISCUSSION

#### 3.1. CdS THIN FILMS

##### 3.1.1. CdS Thin Film Deposited on Polyethylene Terephthalate (PET)

CdS thin film deposited onto PET showed good adhesion and in light yellowish color. Besides this, as can be seen in Figure 3.1, all CdS thin films were molecularly homogenous and pin-hole free. Figure 3.1 also shows that, as the deposition temperature is lowered from 110°C to 90°C, surface of the CdS films becomes smoother. EDX analysis was used to investigate the relationship between process conditions and Cd:S atomic ratio. It was observed that for all deposition temperatures Cd:S atomic ratios were very close to 1:1 (Figure 3.1 (d)-(f)).

X-ray diffraction analysis (Figure 3.2) showed that all the samples (both on PET and glass) have a strong peak around 26° (2 $\theta$ ). This peak can be assigned to the (002) hexagonal or (111) cubic CdS structure. Also there is a minor peak around 54° (2 $\theta$ ), which could be attributed to the (311) cubic CdS structure. Another fact is that, this peak could either come from PET or CdS. Depending on the process conditions, such as deposition and annealing temperature, crystal structure of PET changes. It is very difficult to identify the CdS peak from X-ray diffraction pattern of CdS thin films deposited on ITO coated PET. Therefore, CdS thin films on ITO coated glass substrate are grown under the same experimental conditions. Similar to the CdS thin films deposited on ITO coated PET, for the CdS thin film deposited on ITO coated glass a strong peak around 26° (2 $\theta$ ) has been observed (Figure 3.2 (b)). Moreover, no significant peak for the substrate has been observed. Hence, it is possible to conclude that for both PET and glass substrates, 26° (2 $\theta$ ) can be

assigned to CdS and CdS was in hexagonal structure with the preferred orientation along (002) direction.

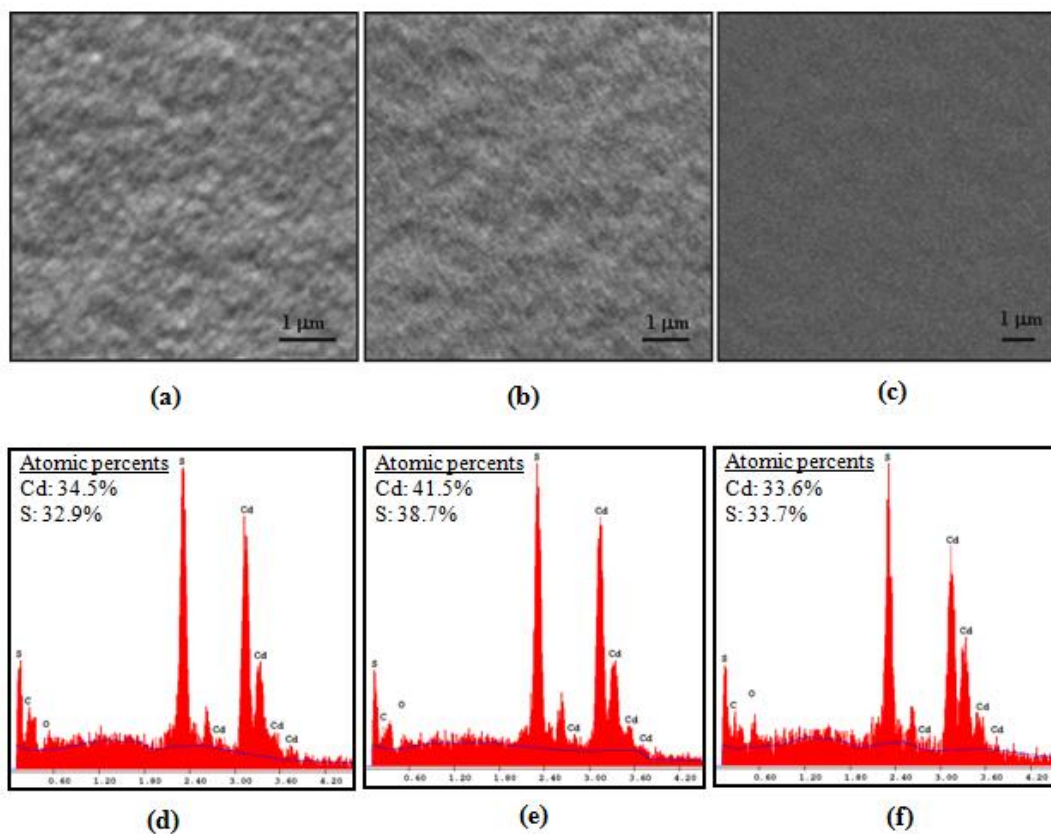


**Figure 3.1.** SEM pictures and EDX analysis results of CdS thin films deposited onto ITO PET under 3V bias for 20 min at (a)-(d) 110 °C, (b)-(e) 100°C and (c)-(f) 90°C

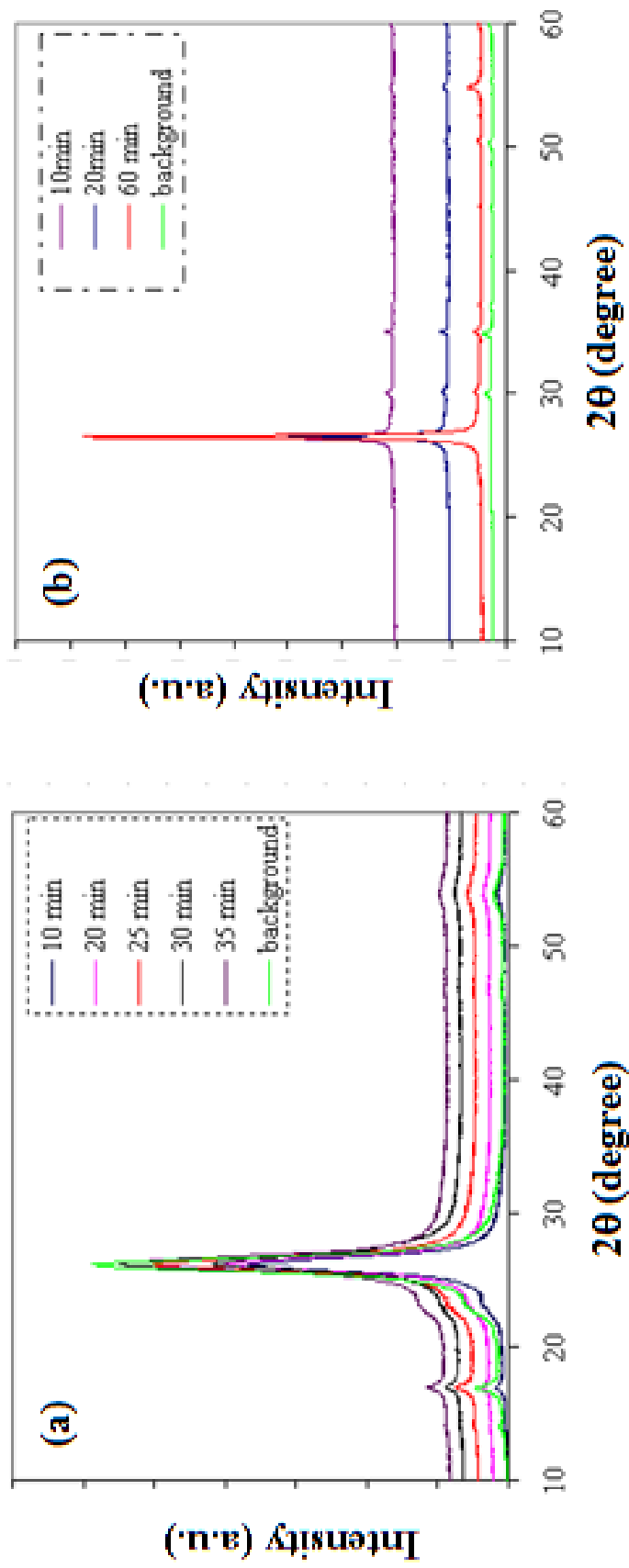


**Figure 3.2.** X-ray diffraction pattern of CdS thin films growth on (a) ITO coated PET and, (b) ITO coated glass for various times

Grain size of the CdS thin films was calculated using the well known equation [78];

$$d = \frac{\lambda}{\beta \cos\theta}$$

where,  $d$  is the crystal size;  $\lambda$  is the X-ray wavelength used;  $\beta$  the angular line width of half maximum intensity;  $\theta$  is the Bragg's angle. The average grain size of the samples is around 6.5 nm indicating the nanocrystalline structure. Grain size of the samples decreased from 6.7 to 6.4 nm while the deposition temperature increases from 90 to 110 °C. The effect of deposition time on grain size was also investigated. For this purpose, deposition temperature kept constant at 100 °C, while the deposition time changed from 5 to 30 min (Table 1). In this case, like the effect of deposition temperature, a slight change in grain size was obtained with increasing the deposition time. The grain size decreased from 6.6 to 6.3 nm while the deposition time goes from 5 to 30 min.

**Table 1** Effect of deposition temperatures and time on grain size

Deposition Temperature (°C)	Deposition Time (min)	Grain Size (nm)	$E_g$ (eV)
90	20	6.7	2.75
	30	6.3	2.68
100	20	6.3	2.67
	10	6.5	2.68
	5	6.6	2.66
110	20	6.4	2.62

The effects of deposition temperature and time on optical properties of the CdS films were investigated in this study. Figure 3.3 (a) indicates all PET samples have very high optical transmittance in the wavelength region greater than 500nm. An oscillatory behavior has been obtained for  $\lambda > 500$  nm due to the interference fringes produced by the reflected light waves from two surfaces of thin film. The optical band gap energy  $E_g$  was calculated from the following variation of the absorption coefficient ( $\alpha$ ) with photon energy [79];

$$(\alpha h\nu) = A(h\nu - E_g)^n$$

where A is a constant, and n is the power exponent, which takes 1/2 value for direct allowed transition and 2 for indirect allowed transition. As seen in Figure 3.3 (b), for all samples, the change of  $(\alpha h\nu)^2$  versus photon energy  $h\nu$  with  $n=1/2$  have very good linearity indicating that the optical transition in CdS thin films is direct allowed transition. The extrapolation of the straight line of  $(\alpha h\nu)^2$  versus photon energy allows obtaining the band gap energy values.

Table 1, summarizes all band gap energy data for CdS thin film deposited on PET. The highest band gap value, which is 2.75 eV, was obtained for the sample deposited at 90 °C for 20 min. On the contrary, the lowest band gap value, which is 2.62 eV, was obtained for the sample deposited at 110 °C for 20 min. All these values are greater than the band gap of bulk CdS, which is 2.42 eV. The reason of this blue shift could be attributed to the quantum size effect in CdS nanocrystal. Similar effect for the CdS nanocrystalline thin films deposited onto glass substrate using chemical bath deposition technique was reported [80].

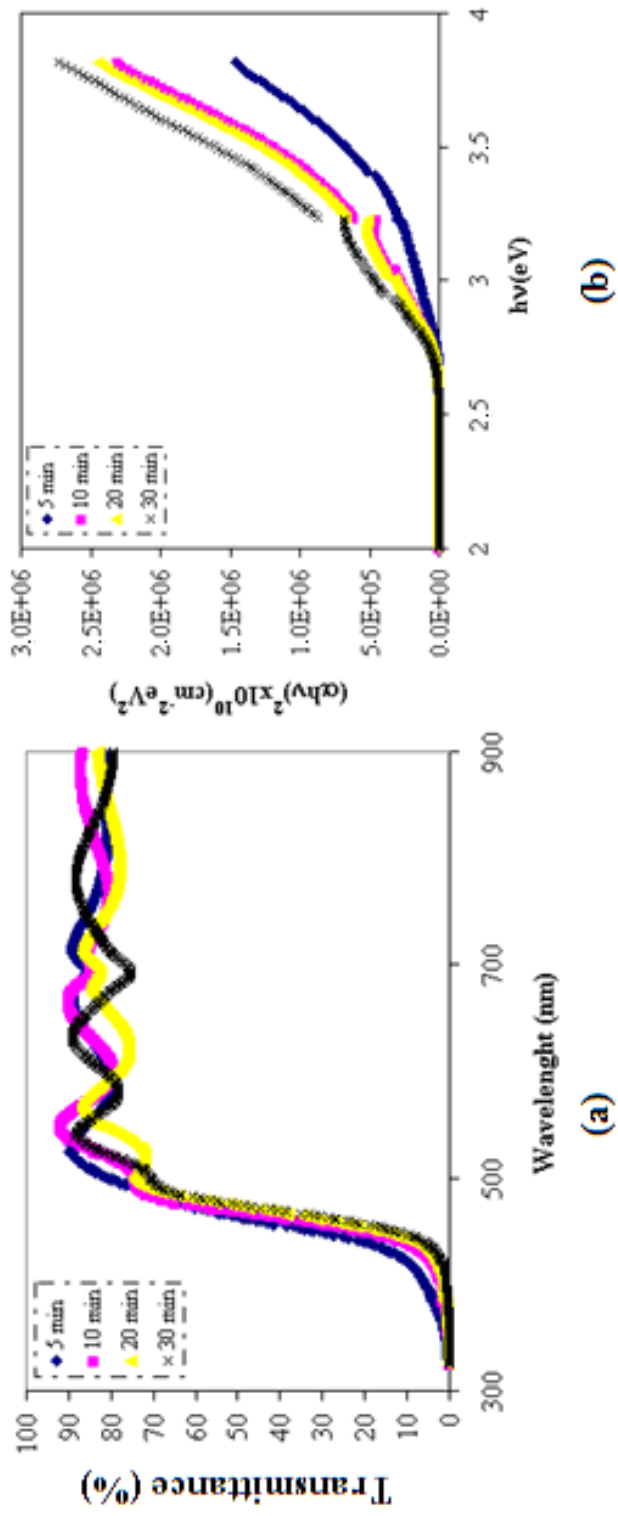


**Figure 3.3.** (a) Transmittance, (b)  $(\alpha h\nu)^2$  versus photon energy  $h\nu$  plot of CdS thin films deposited onto ITO coated PET at 100°C, under 3V bias for different deposition time.

### 3.1.2. Photoelectrochemical and Electrochemical Impedance Performances of CdS Thin Films and the Effect of CuCl<sub>2</sub> Treatment on CdS Thin Films

Previously deposited CdS thin films on PET substrates were immersed into 5mM CuCl<sub>2</sub> aqueous solution for 2 minutes at room temperature. Then films were let to dry at room temperature for 24 hours.

Photoelectrochemical (PEC) cell configuration was formed with CdS thin film as working electrode into a three-electrode one compartment cell, with a graphite counter electrode and Ag/AgCl reference electrode. Figure 3.5 represents the photoelectrochemical cell (PEC) configuration formed with three-electrode cell for the photoelectrochemical and electrochemical impedance measurements. Electrical response of the CdS under illumination (35 mW/cm<sup>2</sup>) has been recorded using a Gamry G750 Potentiostat/Galvanostat/ZRA system. 0.1M Na<sub>2</sub>S, 0.1M NaOH and 0.1M S solution has been used as electrolyte. For electrochemical impedance measurement the same experimental conditions and setup was used.

As-deposited CdS thin films have high optical transmittance (>80%) for the wavelengths greater than 500 nm as mentioned in the previous part. As can be seen in Figure 3.4 (a), after post treatment, a decrease in transmittance has been observed. The maximum transmittance of the CuCl<sub>2</sub> treated samples changed between 50 and 60% depending on the deposition time. As seen in Figure 3.4 (b), similar to the as-deposited samples, the change of  $(\alpha h\nu)^2$  versus photon energy  $h\nu$  with  $n=1/2$  have a linearity indicating that the optical transition in CuCl<sub>2</sub> treated CdS thin films is direct allowed transition. The extrapolation of the straight line of  $(\alpha h\nu)^2$  versus photon energy allows us to obtain  $E_g$  values.

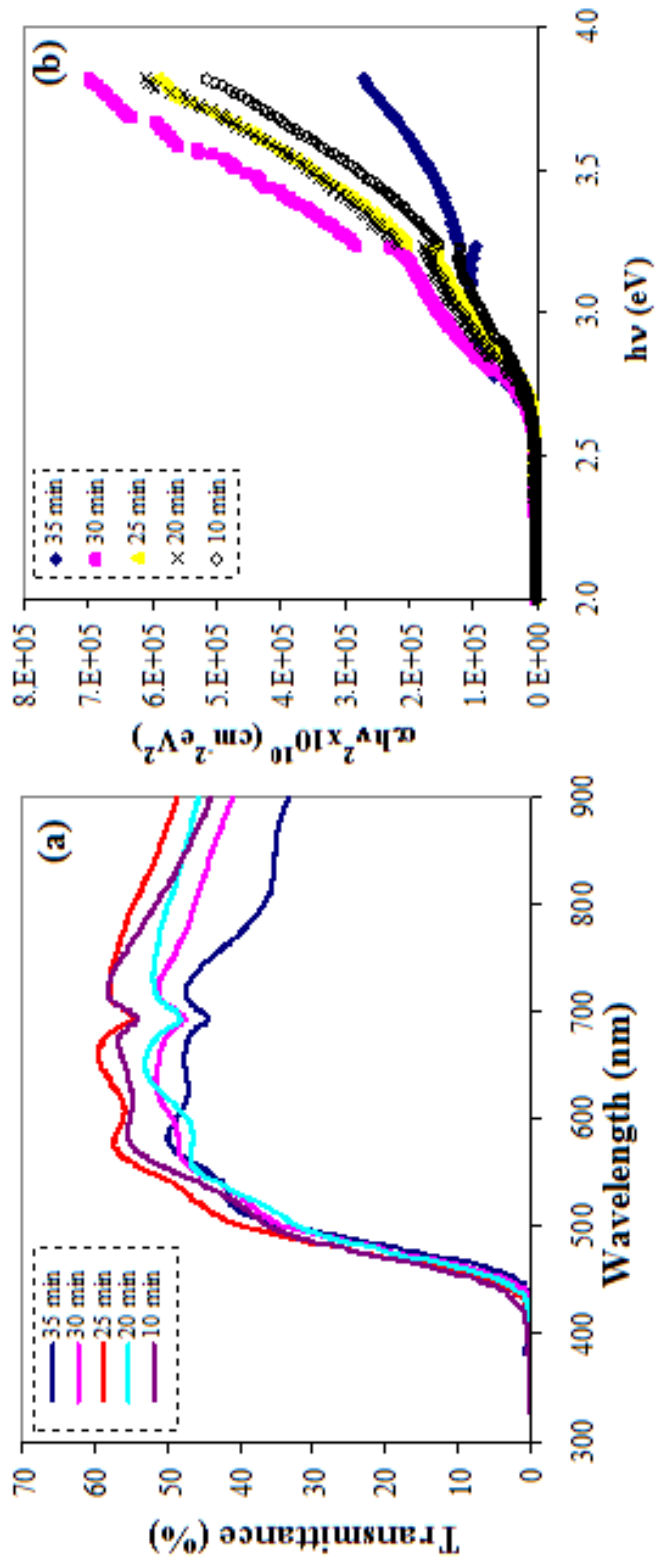


**Figure 3.4.** (a) Transmittance versus wavelength and, (b)  $(\alpha h\nu)^2$  versus photon energy  $h\nu$  plot for the CuCl<sub>2</sub> treated CdS thin films growth for different time intervals

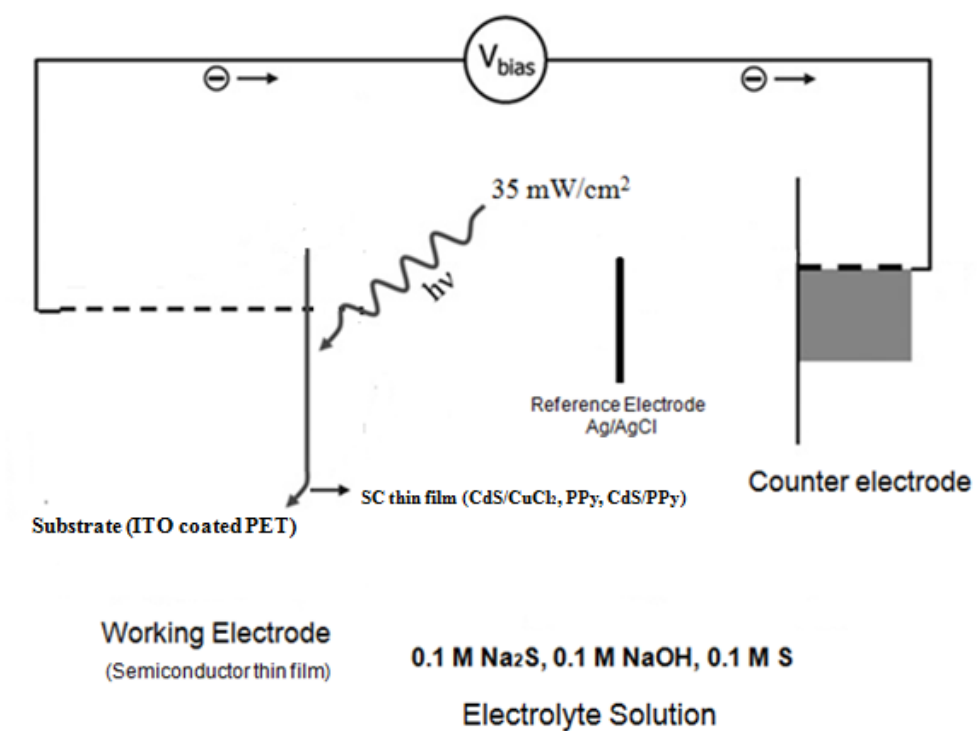


**Figure 3.5** Photoelectrochemical cell configuration with three-electrode cell

Table 2, summarizes the maximum transmittance and  $E_g$  data. Although, there is an increase in both transmittance and  $E_g$  for the sample deposited for 25 min, in overall it is possible to conclude that, both transmittance and  $E_g$  of CdS thin films decreased slightly with increasing the deposition time. It is also worth to mention here that there is a very slight decrease in  $E_g$  of  $\text{CuCl}_2$  treated samples compared to that of as-deposited CdS thin films.

**Table 2** Maximum optical transmittance and band gap energy data for the  $\text{CuCl}_2$  treated CdS thin films deposited for different times

<b>Deposition time (min)</b>	<b>Maximum Transmittance (%)</b>	<b>Band Gap Energy (eV)</b>
10	58	2.66
20	53	2.63
25	60	2.71
30	53	2.63
35	50	2.56

Figure 3.6 shows the current density versus potential graphs under illumination. Fill factor (FF) of the samples were calculated using the very well known equation [81];

$$FF(\%) = \frac{I_{\max} V_{\max}}{I_{sc} V_{oc}} \times 100$$

where,  $I_{\max}$  and  $V_{\max}$  is maximum current and voltage respectively,  $I_{sc}$  is the short circuit current, and  $V_{oc}$  is the open circuit potential. Another identifying factor for the PEC solar cell is the power efficiency, which is equal to the percentage of the

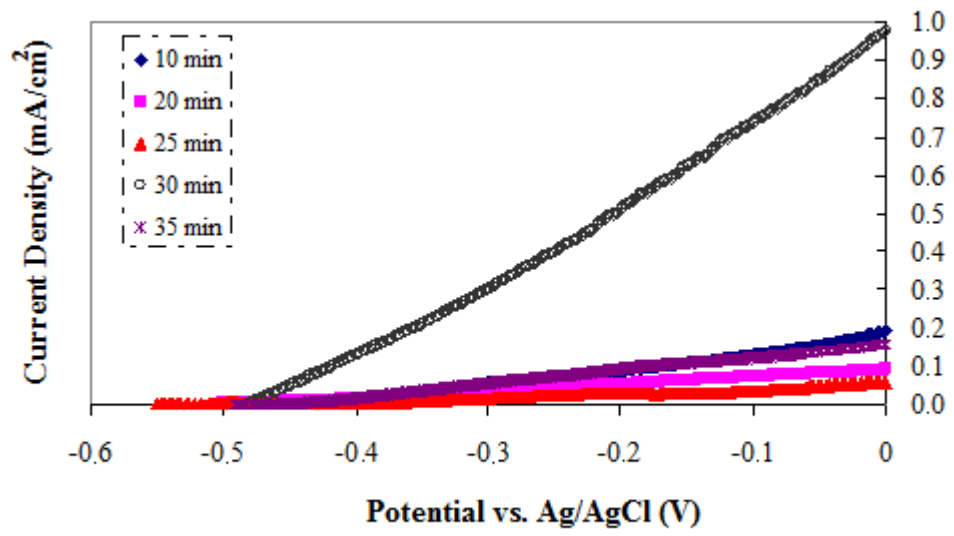
power converted from the absorbed light to the electricity. Hence, power efficiency ( $\eta$ ) can be calculated from [82];

$$\eta(\%) = \frac{I_{\max}V_{\max}}{P_iA}$$

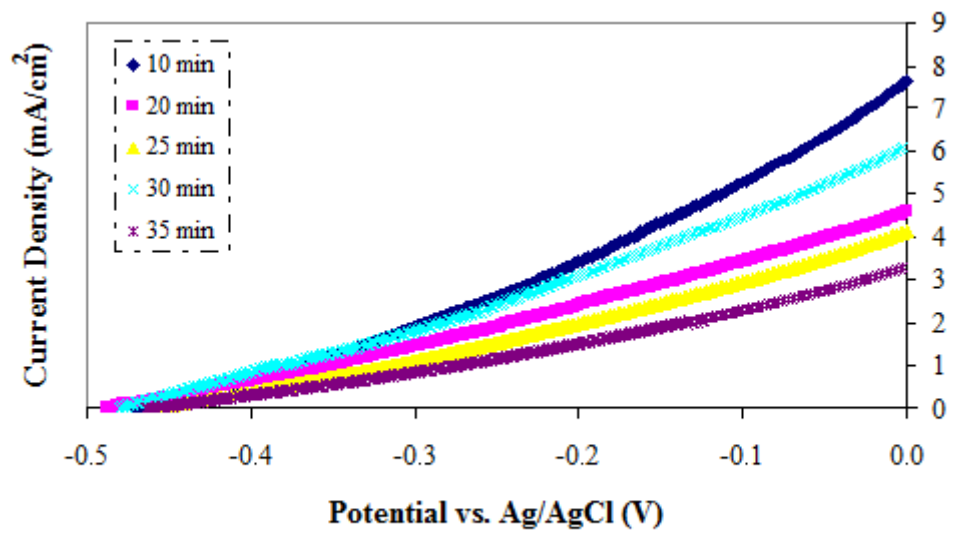
Where,  $P_i$  is the power of incident light and  $A$  is the area of the electrode. The maximum short circuit current ( $I_{sc}$ ), which was about 1.0 mA, has been obtained for the films grown for 30 minutes. For other deposition time, approximately 10 times lower  $I_{sc}$  value has been observed. This indicates the good quality film formation at 30 min. A similar effect of the deposition time on PEC performance has been reported by Kokate et al. for electrochemically deposited CdTe thin films [83]. Table 3 summarizes open circuit potential, short circuit current, fill factor and power efficiency of both as-deposited and  $CuCl_2$  treated CdS thin films.

**Table 3** Photoelectrochemical parameters of CdS thin films

Time (min)	Condition	$I_{sc}$ (mA/cm <sup>2</sup> )	$V_{oc}$ (mV)	FF (%)	$\eta$ (%)
10	As deposited	0.19	452	22	0.05
	$CuCl_2$ treated	7.65	470	19	1.95
20	As deposited	0.09	500	24	0.03
	$CuCl_2$ treated	4.55	487	22	1.39
25	As deposited	0.06	514	23	0.02
	$CuCl_2$ treated	4.10	457	21	1.14
30	As deposited	0.98	480	22	0.29
	$CuCl_2$ treated	6.07	480	22	1.86
35	As deposited	0.16	476	26	0.06
	$CuCl_2$ treated	3.28	461	20	0.86



(a)



(b)

**Figure 3.6.** Current density-Voltage characteristic of (a) as deposited, (b) CuCl<sub>2</sub> treated CdS thin films

As can be seen in Figure 3.6 (b) after  $\text{CuCl}_2$  treatment, short circuit current increased dramatically for all deposition time. The highest maximum power efficiency of the thin films before  $\text{CuCl}_2$  treatment was 0.29% for the sample growth for 30 min, which increased to 1.86% after treatment. The highest power efficiency obtained in this study was 1.95% for the sample growth for 10 min. This is one of the highest power efficiencies reported in literature for the chemically deposited CdS thin film [84-88].

For further characterization of the CdS thin films, frequency dependent measurements were performed using Gamry G 750 Potentiostat/Galvanostat/ZRA system. For this purpose, Mott-Schottky analysis has been carried out under the same experimental conditions with PEC measurements at 50Hz and 100Hz for as-deposited and  $\text{CuCl}_2$  samples respectively. In Mott-Schottky plots, donor density ( $N_D$ ) and the flat band potential ( $E_{fb}$ ) of the samples can be calculated from the linear extrapolation of  $1/C^2$  versus potential graphs [89]. As can be seen in Figure 3.7, there is a tendency to increase in  $1/C^2$  value for the  $V \geq 0V$ , indicating all our samples are n-type. Since the slope of the Mott-Schottky plot is inversely proportional to the  $N_D$ , it is possible to conclude that  $N_D$  of the  $\text{CuCl}_2$  treated samples is higher than as-deposited samples. This indicates the abundance of surface states and/or contribution of double layer capacitance for treated samples. Higher  $N_D$  could be attributed as the reason for high power efficiency of  $\text{CuCl}_2$  treated sample.

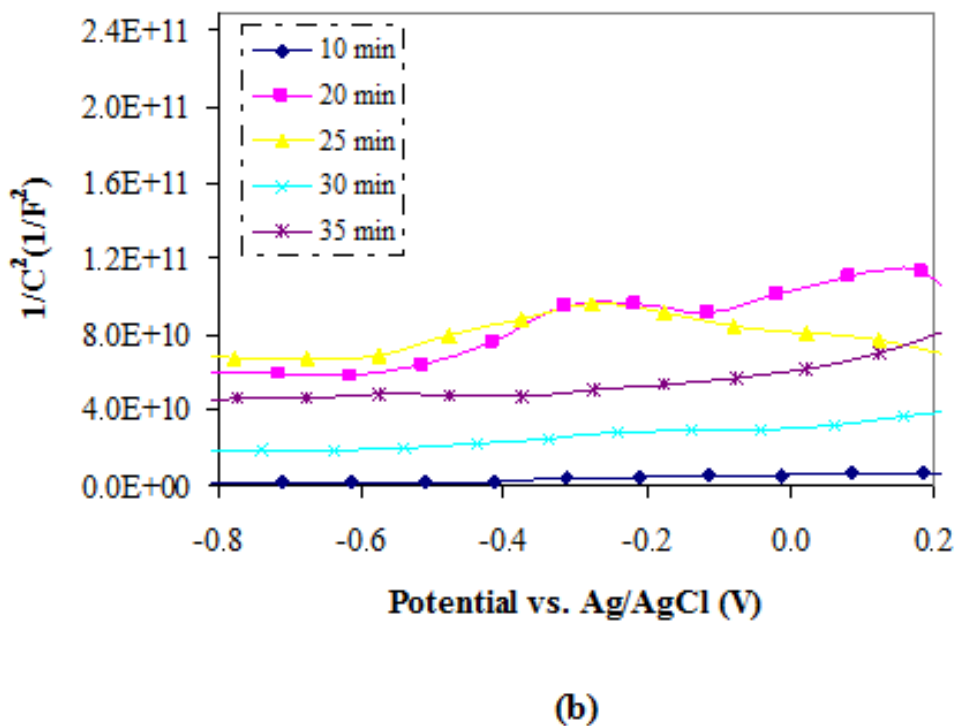
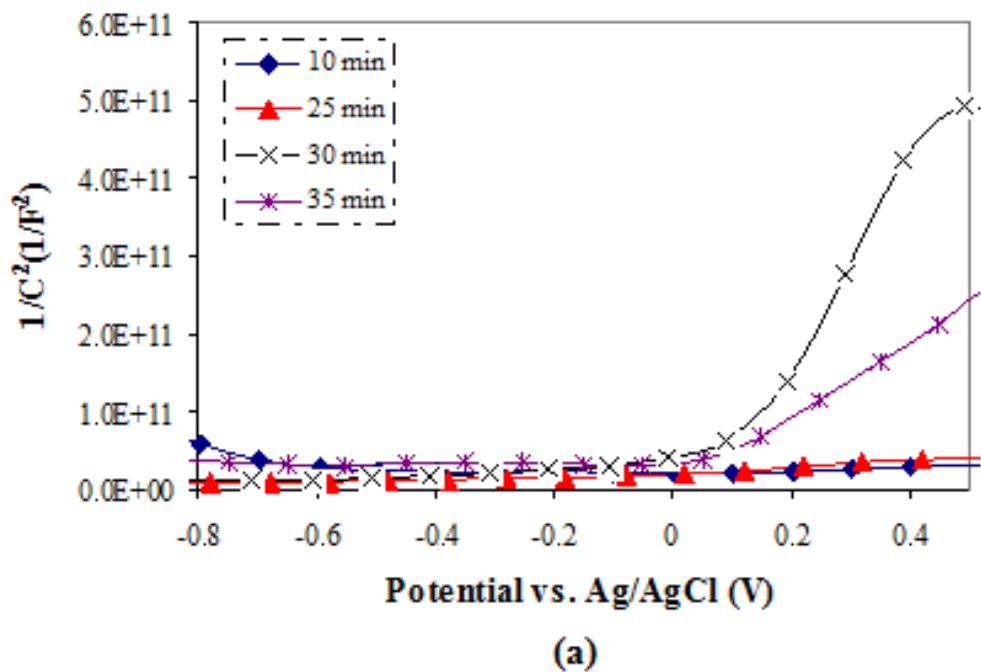


**Figure 3.7.** The Mott–Schottky plot of (a) as deposited, (b) CuCl<sub>2</sub> treated CdS electrode in sulfate electrolyte under 35 mW/cm<sup>2</sup> illumination.

Charge transfer process across the CdS-electrolyte interface was further revealed through electrochemical impedance spectroscopy. Measurements have been performed between 0.01 Hz and 1 kHz. Higher frequency measurements can not be performed due to the small signal/noise ratio. Although, CuCl<sub>2</sub> treatment provided better quality films, CdS thin films suffer from instability in sulphate electrolyte even for high pH values (~12 pH). Therefore, there are deviations from standard models. However, there is a pronounced difference between frequency dependencies of as-deposited and CuCl<sub>2</sub> treated samples. Figure 3.8 shows the Nyquist plots of CdS thin films deposited in this study.

For as deposited samples, except 30 min deposition time, all Nyquist plots of the CdS thin films were nearly semicircle indicating one time constant. However, for 30 min as-deposited sample and all CuCl<sub>2</sub> treated samples exhibit a non-ideal capacitance behavior. It is possible to conclude the charge transfer for these samples was controlled by mixed kinetic and diffusion [90]. In this case, there is extra impedance known as Warburg impedance, which is in series with polarization resistance. For low frequencies, Warburg impedance appears as a straight line. As can be seen in Figure 3.9, after CuCl<sub>2</sub> treatment, polarization resistance decreased significantly. Beside these, electrochemical impedance of our samples decreased approximately 100 times after CuCl<sub>2</sub> treatment (Figure 3.9). This implies that admittance of the as-deposited samples smaller than that of CuCl<sub>2</sub> treated ones, which means as-deposited samples have smaller constant phase element capacitance.

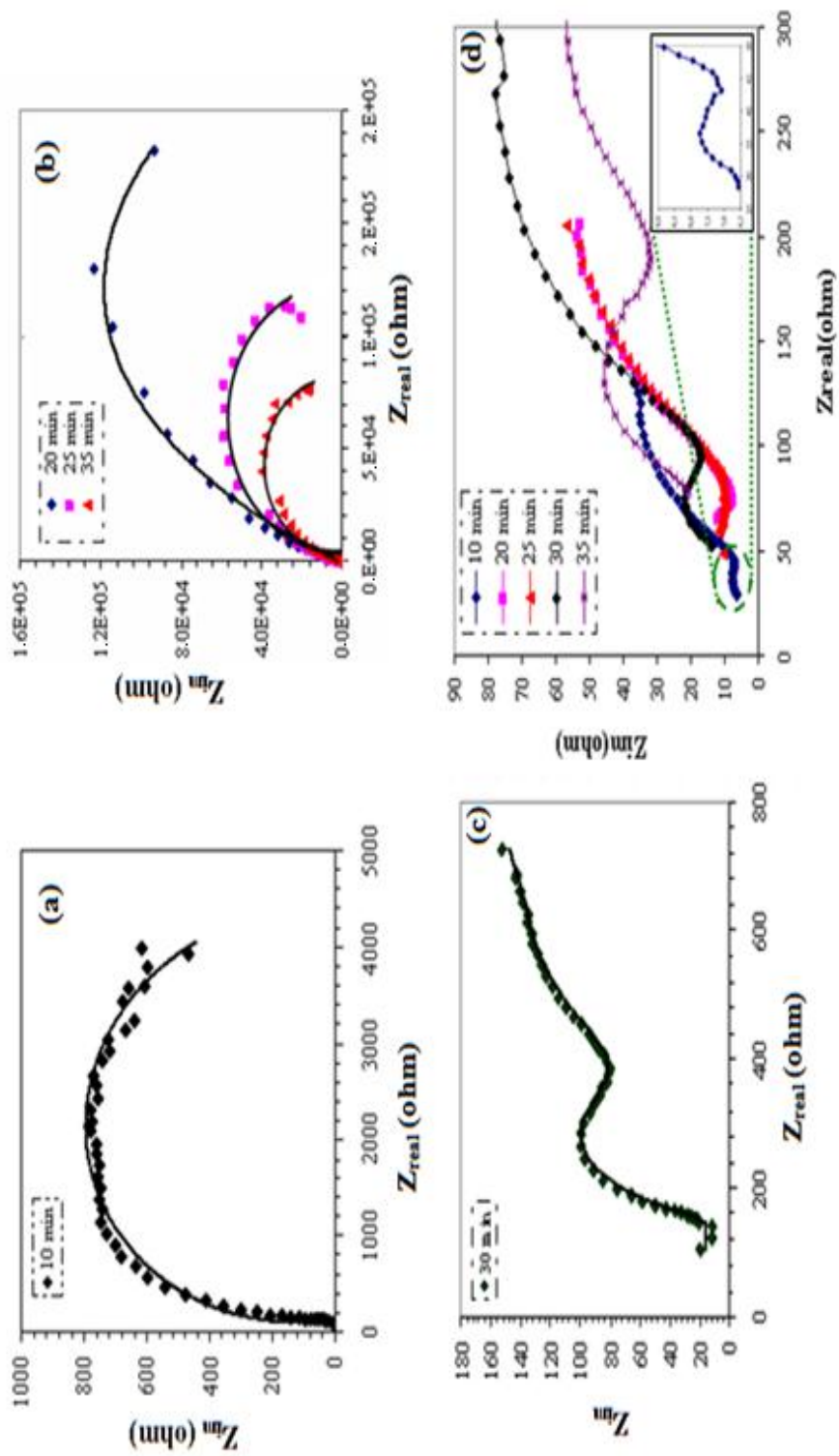
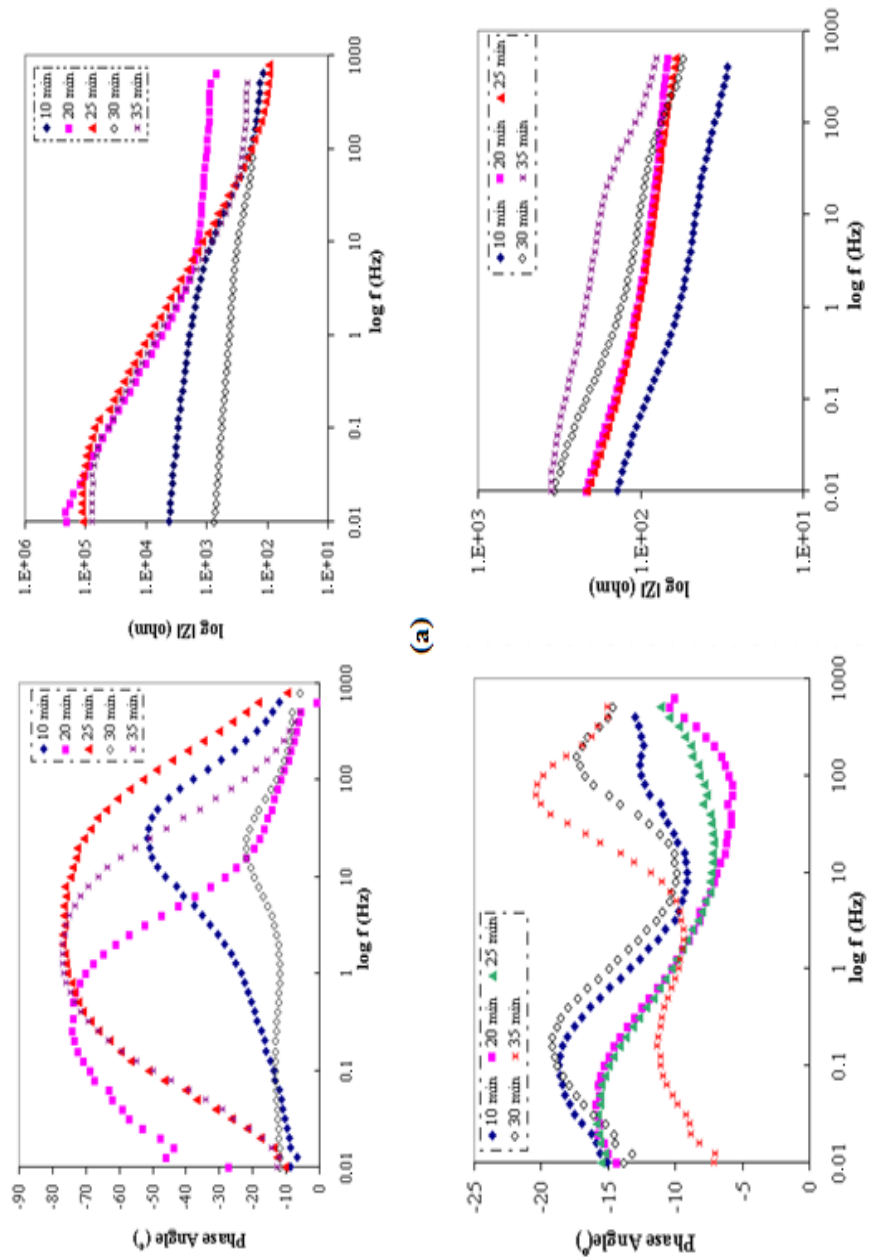


Figure 3.8. Nyquist plots of (a)-(c) as-deposited CdS thin films, (d) CuCl<sub>2</sub> treated samples



**Figure 3.9.** Bode plots of (a) as-deposited and (b) CuCl<sub>2</sub> treated CdS thin films

### 3.1.3. CdS Thin Films Deposited on Soda Lime Glass Substrates

CdS thin films were also deposited on ITO coated soda lime glass substrates. Similar with the thin films deposited on PET substrates, these films were also adherent, in light yellowish color, homogenous and pinhole free as can be seen from SEM pictures (Figure 3.10).

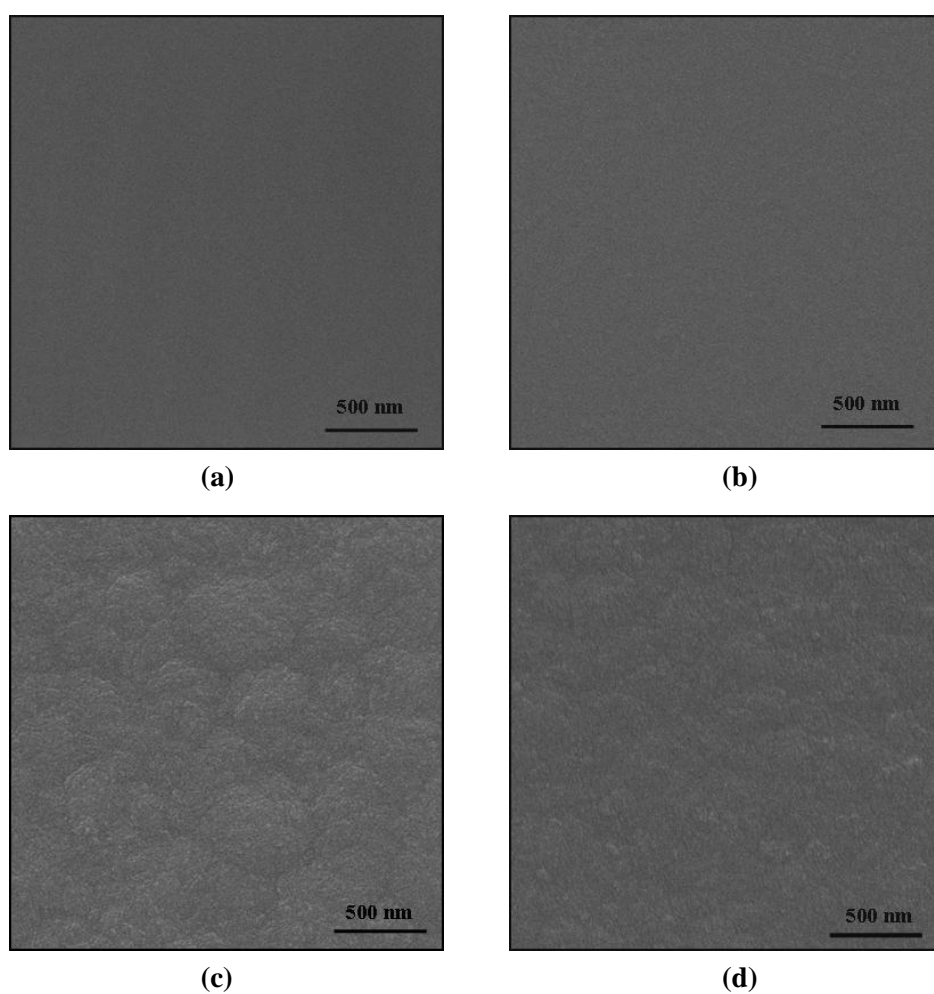


**Figure 3.10.** SEM pictures of CdS thin films deposited at 125 °C for (a) 60 min, (b) 30 min, (c) 20 min, and (d) 10 min on ITO coated soda lime glass substrates.

Compositional and structural properties of the films were investigated by EDX and X-Ray analysis. EDX analysis was used to investigate the relationship between deposition time and Cd:S atomic ratio. It was observed that Cd:S atomic ratio increased from 0.8 to 1.1 with increasing deposition time (Figure 3.11).

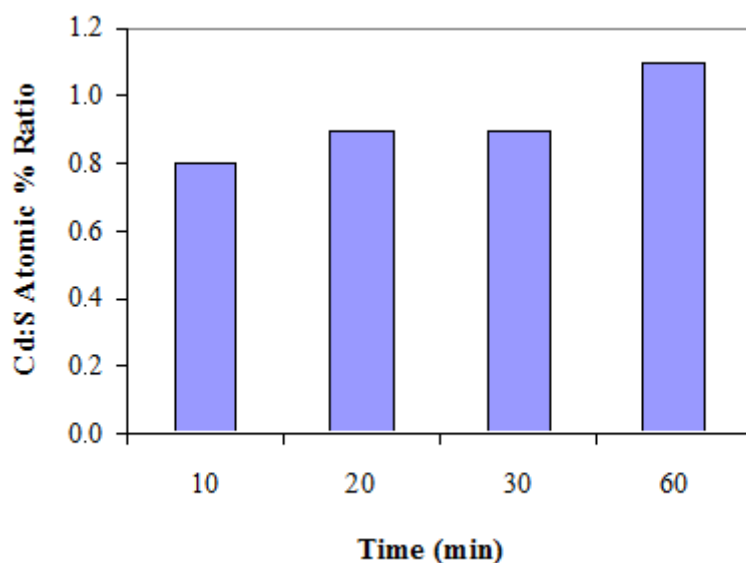


**Figure 3.11.** Relationship between deposition time and Cd:S atomic ratio

X-ray diffraction analysis (Figure 3.12) showed that all the samples have a strong peak around  $26^\circ$  ( $2\theta$ ). This peak can be assigned to the (002) hexagonal or (111) cubic CdS structure. Since no other significant diffraction peaks have been found in the samples deposited on glass substrates, it is again possible to conclude that samples have a hexagonal CdS structure with the preferred orientation along (002) direction. An increase in the intensity of the reflection peaks was observed for the samples which were annealed at 150, 250 and 350 °C (Figure 3.13). It is possible to say that, the reason for the increase in the intensity of the peaks after annealing could be related with the effect of annealing on the crystallinity of the films.

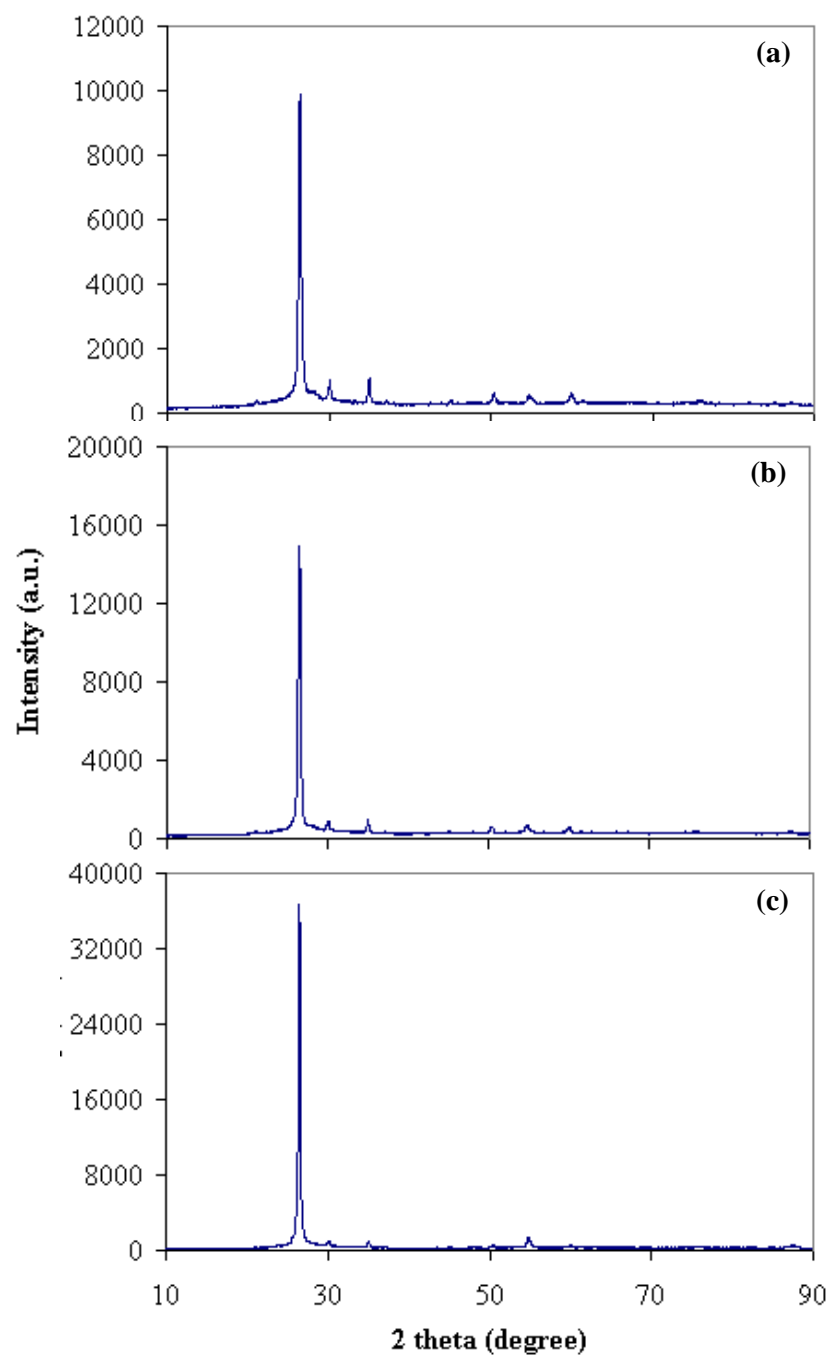


**Figure 3.12.** X-ray diffraction patterns of CdS thin films deposited onto ITO coated glass substrate at 125 °C for a) 10 min b) 20 min, and c) 30 min

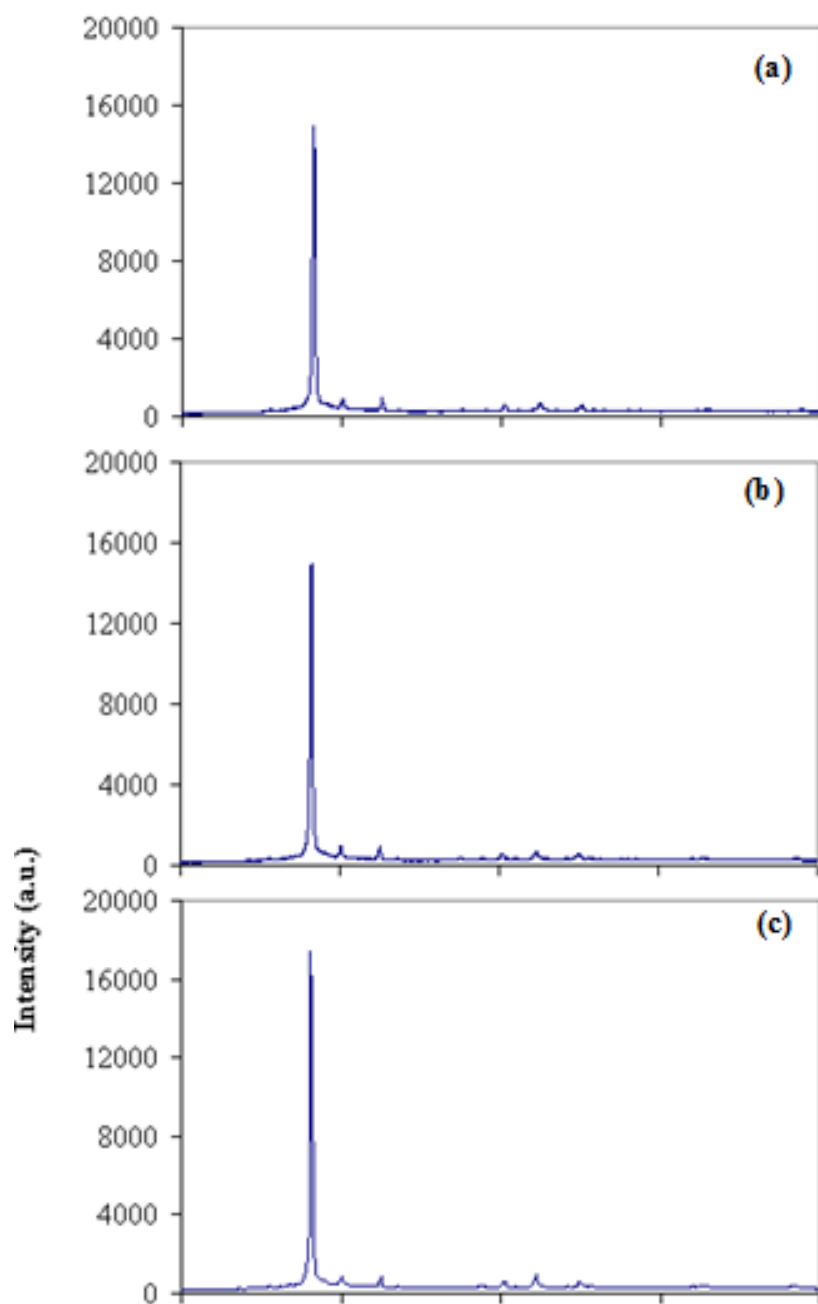


**Figure 3.13.** X-ray diffraction patterns of CdS thin films deposited onto ITO coated glass substrate at 125 °C for 10 min and annealed at a) 150, b) 250, and c) 350 °C

Grain size of the samples increased with increasing deposition time (Figure 3.14). The maximum grain size for the sample deposited for 60 minutes was found to be 45.55 nm. Grain size of the sample deposited for 10 minutes was found to be 35.02 nm.

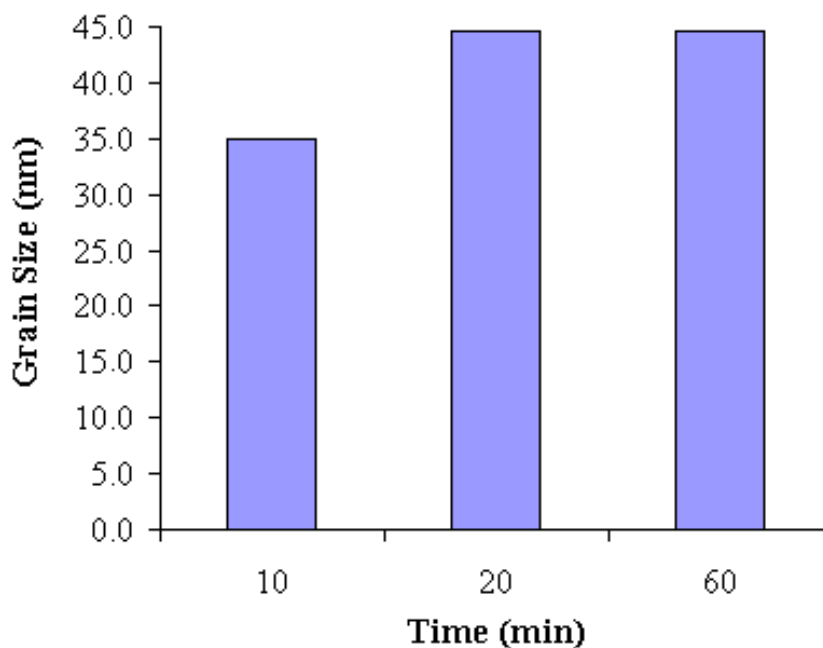


**Figure 3.14.** Relationship between grain size of the films and deposition time.

The effects of deposition time on optical properties of the CdS films were investigated in this study. Figure 3.15 indicates that all samples deposited on ITO coated glass substrates have very high optical transmittance in the wavelength region greater than 500nm.

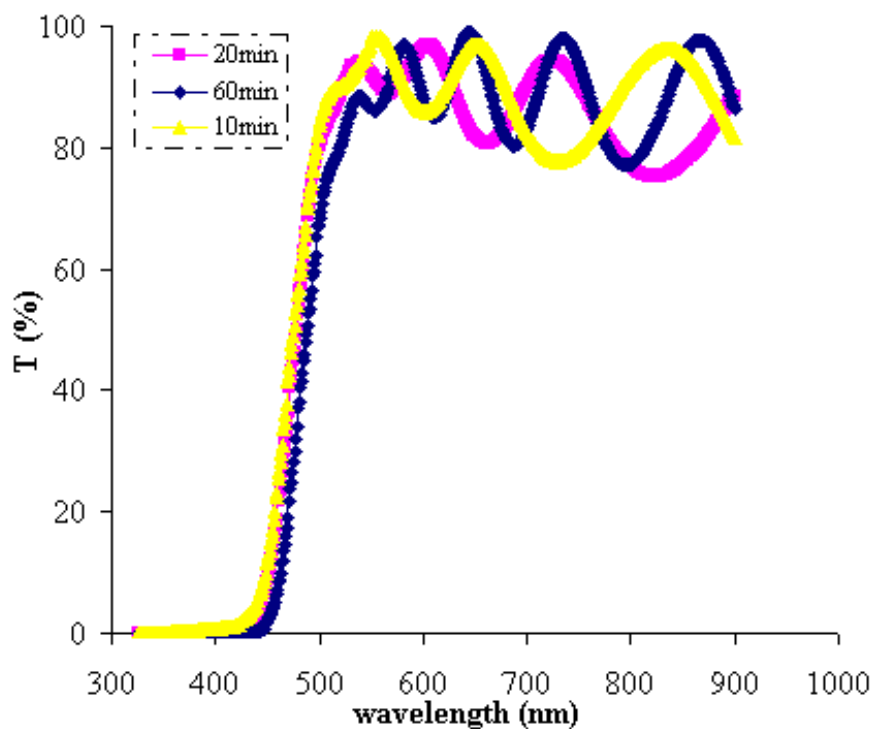


**Figure 3.15.** Transmittance versus wavelength plot of CdS thin films deposited onto ITO coated glass substrates at 125°C, for three different deposition time.

As can be seen from Table 4 band gap energies of the CdS thin films varied from 2.53 to 2.68 eV due to the deposition conditions. Table 4 also shows that the band gap energies of the films decreased for the samples deposited under nitrogen atmosphere. The lowest band gap achieved belonged to the sample deposited under nitrogen atmosphere for 20 minutes (2.49 eV). As a result of a higher crystallinity obtained by annealing process, it was observed that it is possible to achieve lower band gap energies by annealing the films deposited on glass substrates after deposition. Table 5 summarizes the band gap energies of the samples annealed at various temperatures. Band gap energy of the sample annealed at 350 °C was found to be 2.42 eV which is the band gap value of bulk CdS.

**Table 4** Band gap energies of CdS thin films deposited onto ITO coated soda-lime glass at 125°C

<b>Nitrogen Flow</b>	<b>Deposition Time (min)</b>	<b>E<sub>g1</sub> (eV)</b>
	60	2.68
No	20	2.53
	10	2.68
Yes	60	2.60
	30	2.49
	10	2.67

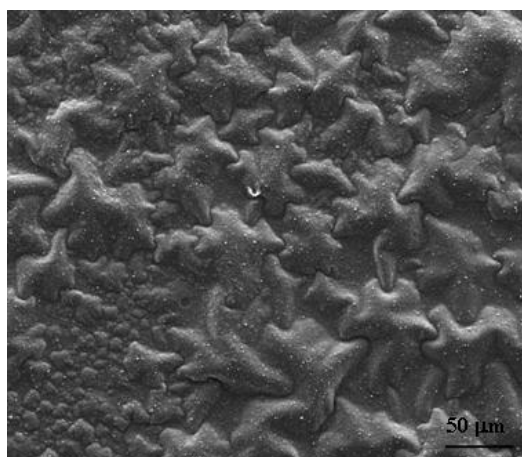
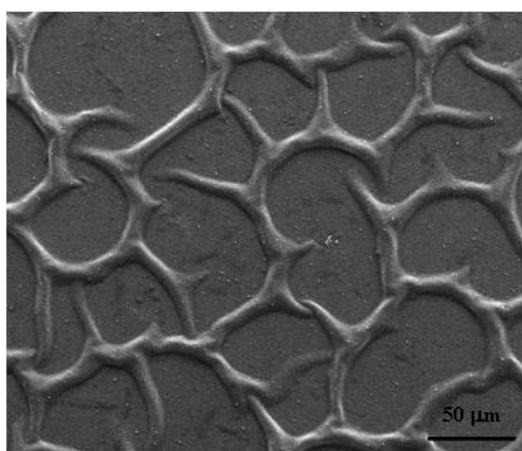
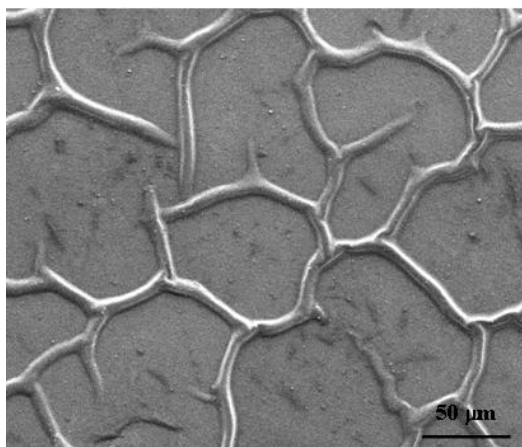
**Table 5.** Effect of annealing on band gap energy of CdS thin films deposited onto ITO coated soda-lime glass at 125 °C, 3V for 20min.

<b>Annealing Temperature (°C)</b>	<b>E<sub>g1</sub> (eV)</b>
As deposited	2.53
150	2.62
250	2.46
350	2.42

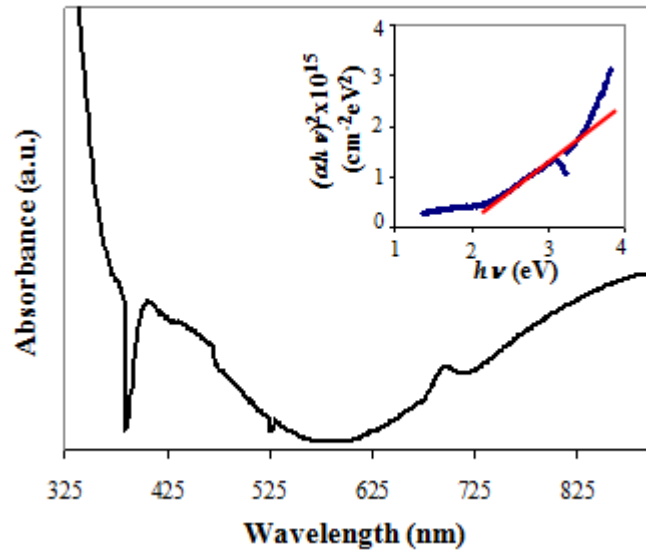
### 3.2. PPy and CdS/PPy THIN FILMS

Figure 3.16. shows the SEM pictures of PPy thin films on ITO-PET substrate at room temperature for various deposition times. As can be seen in this figure, increase in deposition time results rough surface. During the deposition, thin films had a tendency to peel off from the surface for higher deposition time. However, after the films were dried, they adhered very well on the surface. The maximum deposition time for the PPy on PET has been determined as 5 min.

UV-vis spectra of the PPy thin film growth on ITO-PET substrate can be seen in Figure 3.17. Two characteristics absorption peaks around 390 and 590 nm were observed for the investigated thin films, which were also shown in previous studies [91]. Aforementioned, the band gap of the CdS thin films directly deposited on ITO-PET at 100 °C for 30 min was 2.7 eV. Similar to the CdS thin films,  $E_g$  of the PPy thin films, which is around 2.0 eV , was calculated using the extrapolation of the straight line of the  $(\alpha h\nu)^2$  versus photon energy plot (Figure 3.17.).



**Figure 3.16.** SEM pictures of Ppy thin films grown on ITO-PET at room temperature for (a) 30 sec, (b) 1 min, (c) 5 min



**Figure 3.17.** UV-vis spectra of Ppy thin film grown for 1 min on ITO-PET

PEC characteristics of the thin films were performed at room temperature under  $35 \text{ mW/cm}^2$  illumination. Figure 3.18(a) shows the current density versus potential graph of PPy thin film under illumination.  $I_{sc}$  of the samples increased from 0.05 mA to 0.20 mA with increasing the growth time. The average power efficiency of the PPy thin films was 0.02% (Table 6). These values are one of the highest  $I_{sc}$  and  $\eta$  values of the previously reported polymeric thin films. For example, H. Kim et al. have been reported photoelectrochemical behavior of PPy and PPy/platinum nanoparticles in 0.1 M KCl [92]. In that study,  $I_{sc}$  of PPy and PPy/platinum nanoparticles were about 0.5 and 1.0  $\mu\text{A}$  respectively. Also, the maximum photoelectrochemical efficiency of the poly (terthiophene) thin film reported by C.J. Harrison was 0.0063% [93].

**Table 6.** Photoelectrochemical parameters of PPy and PPy/CdS thin films

Time (min)	$I_{sc}$ (mA)	$V_{oc}$ (mV)	FF (%)	$\eta$ (%)	Condition
	0.06	472	29	0.02	PPy
0.5	1.67	444	22	0.47	PPy/CdS
	0.12	192	22	0.01	PPy
1	1.96	454	23	0.58	PPy/CdS
	0.10	382	24	0.03	PPy
3	0.17	436	23	0.05	PPy/CdS
	0.21	156	19	0.02	PPy
5	0.13	394	23	0.04	PPy/CdS

In this study, photoelectrochemical behavior of PPy/CdS thin films was also investigated. For this purpose, CdS thin films were electrochemically deposited on PPy/ITO-PET electrodes. Figure 3.18(b) shows the current density versus voltage graph for the CdS deposited PPy thin films.  $I_{sc}$  of the films grown for 30 sec and 1 min increased dramatically after CdS deposition. The power efficiency of the PPy/CdS films increased up to 0.58% for the sample with 1 min deposition time. Moreover, the stability of the CdS coated PPy thin films were superior compare to the only CdS coated PET electrodes. It is worth to mention here that, power efficiency of the PPy/CdS films was higher than that of the CdS thin films deposited on PET. This improvement could be attributed to the electron-collector behavior of the PPy layer decreasing the losses by recombination and enhancing the photocurrent.

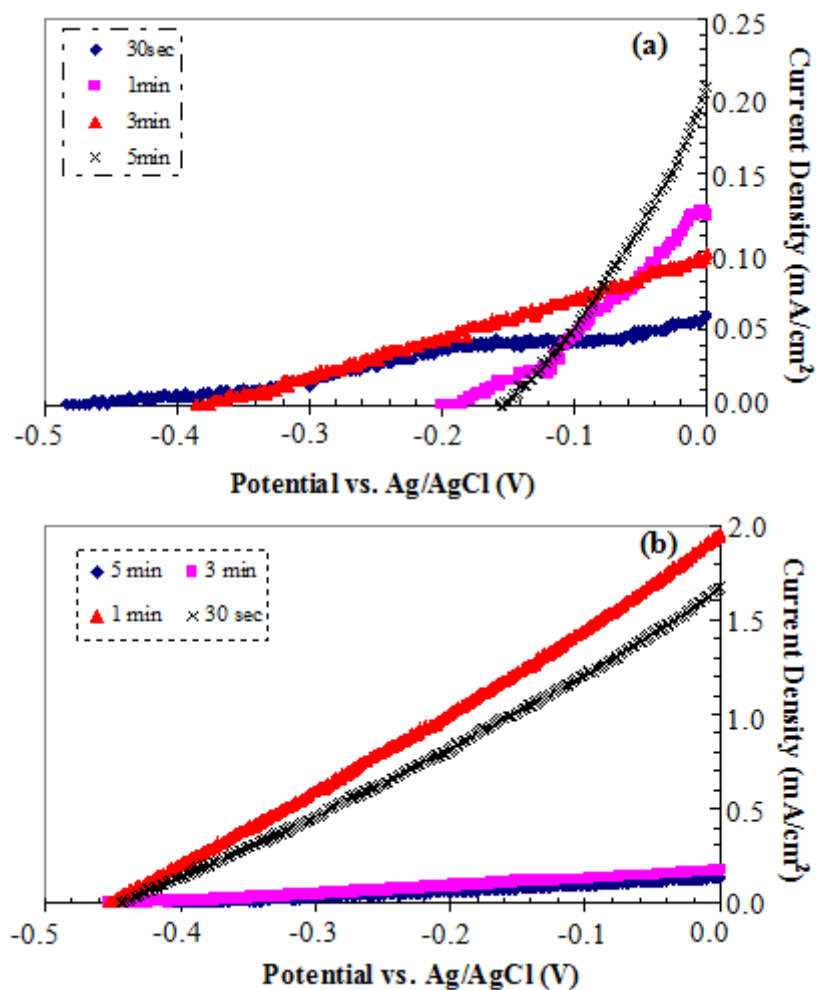


**Figure 3.18.** Current density-Voltage characteristic of (a) Ppy (b) Ppy/CdS thin films deposited on ITO-PET

For further characterization of the PPy and PPy/CdS thin films, frequency dependent measurements were performed using Gamry G750 Potentiostat / Galvanostat / ZRA system. For this purpose, Mott-Schottky (MS) analysis was carried out under the same experimental conditions with PEC measurements at 50 Hz. Basically, MS plot predicts a linear relationship between applied potential and the square of the capacitance arising from the space charge layer in the semiconductor. Depending on the charge carrier type, which can be either electrons

or holes, slope of MS plot can be positive or negative [94]. Therefore, type of semiconductor material can be predicted from MS analysis. Moreover, slope of MS plot is inversely proportional to the effective donor or acceptor concentration in the semiconductor [95]. Figure 3.19 shows the  $1/C^2$  versus potential graph of PPy and PPy/CdS thin film. PPy thin films behave like n-type material for 30 sec, 1 min. and 3 min. deposition time. On the other hand, when the deposition time increased to 5 min. an inverse relationship between  $1/C^2$  and voltage was observed. This indicates the holes or positively charged impurities in the polymer back bone was responsible for the charge transfer. Since the PPy thin film deposited for 5 min. is p-type and the CdS thin films are n-type when these two materials were brought into contact a p-n junction should be formed. The magnitude of the band bending ( $V_{bi}$ ) at the p-n junction can be predicted from the  $x$ -intercept of MS plot. As can be seen in Figure 3.19,  $V_{bi}$  for the PPy-5 min/CdS sample is about 0.71 V. Formation of a p-n junction between p-type organic and n-type inorganic semiconductor has also been reported by Grant C. D. et al [96]

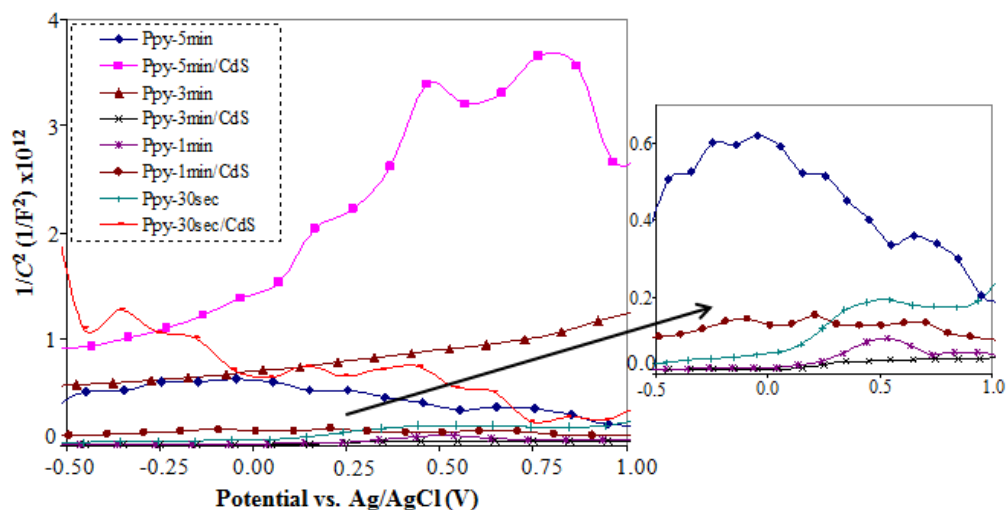
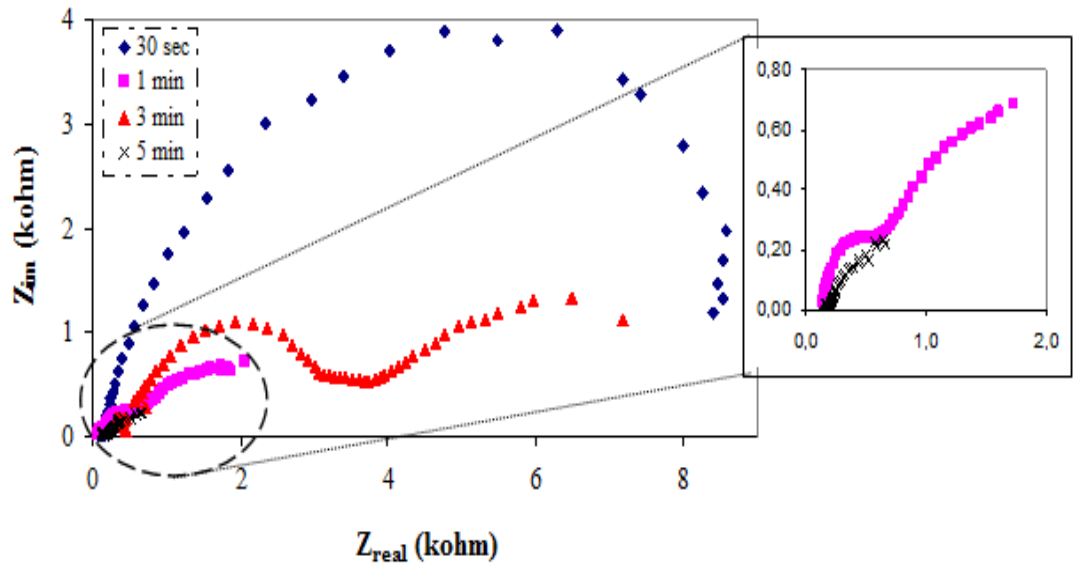
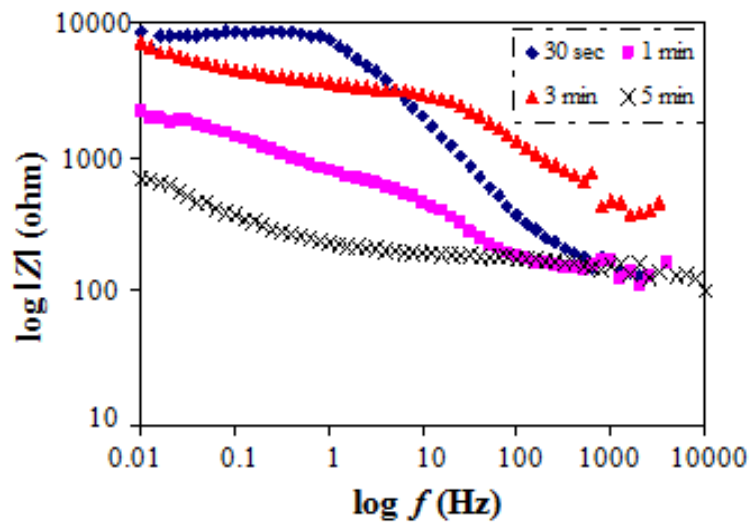


**Figure 3.19.** The Mott–Schottky plot of Ppy and Ppy/CdS electrode

Charge transfer process across the PPy-electrolyte and PPy/CdS-electrolyte interfaces was further revealed through electrochemical impedance spectroscopy. Measurements have been performed between 0.01 Hz and 1 kHz. Figure 3.20(a) shows the Nyquist plots of PPy thin films prepared in this study. Nyquist plot of the sample deposited for 30 sec was nearly semicircle indicating one time constant. However, all other samples indicate two regions of distinct electrochemical response. It is possible to conclude that the charge transfer for these samples was controlled by mixed kinetic and diffusion. A similar behavior of the PPy film deposited on stainless steel has been reported by T. Tuken [97]. Two separate plateau region was observed in  $\log f - \log Z$  plots (Figure 3.20(b)). These two regions reveals that charge transfer resistance of PPy thin films is lower for high frequency range compare to that of low frequency range. It can also be concluded that the sample deposited for 5 min has the minimum charge transfer resistance among the PPy thin films investigated in this study.



(a)



(b)

**Figure 3.20.** (a) Nyquist and (b) Bode plots of Ppy thin films

After CdS deposition, charge transfer of all films were controlled by mixed kinetic and diffusion (Figure 3.21(a)). Unlike the PPy film, charge transfer resistance of the PPy/CdS films increased with increasing the deposition time (Figure 3.21(b)). In addition, the impedance response of the PPy thin films grown for 1 and 5 min. and PPy/CdS thin films grown for 30 sec. and 1 min. at low frequencies disclose reflective finite diffusion to blocking electrode (Figure 3.18 and 3.19). All these results could be attributed to the increase in power efficiency of the PPy films after CdS deposition. Figure 3.20 represents the photoelectrochemical cell (PEC) configuration formed with three-electrode cell for the photoelectrochemical and electrochemical impedance measurements of CdS, PPy and CdS/PPy thin films.

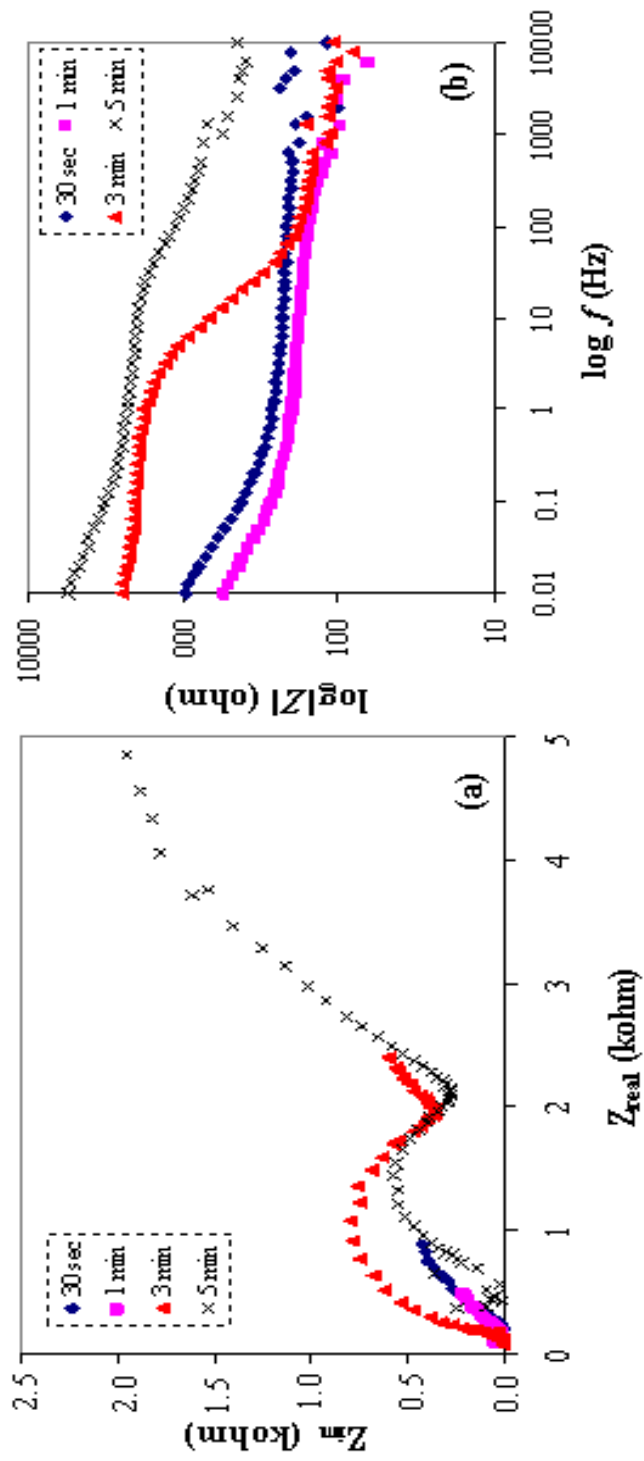


**Figure 3.21.** (a) Nyquist and (b) Bode plot of Ppy/CdS thin film

## CHAPTER 4

### CONCLUSIONS

In this study, CdS thin films were successfully deposited onto mechanically flexible PET substrate via dc-electrochemical deposition technique. Morphological, structural and optical characterizations of the CdS nanocrystal thin films were performed. SEM analysis confirmed that for the selected deposition temperatures and time, all CdS thin films were structurally homogenous and pin-hole free. EDX and X-ray diffraction studies were used to analyze the structure of the thin films. The main Cd and S peaks with the atomic percent ratio close to 1:1 was obtained as observed from EDX results. A hexagonal CdS peak was seen at X-ray diffraction pattern. The average grain size of our PET and glass substrates was around 6.5 and 40 nm, respectively. All the samples have very high optical transmittance for the wavelengths greater than 500 nm, indicating that this is a promising material for a window layer for the flexible solar cell applications. The band gap energies of the films, which range between 2.75 and 2.62 eV, decreased with increasing deposition temperature. It has also been observed that,  $E_g$  of the CdS thin films deposited onto glass substrate decreased with annealing and reached 2.42 eV.

Structural, optical and photoelectrochemical behavior of both as-deposited and  $\text{CuCl}_2$  treated samples was investigated. It was observed that  $\text{CuCl}_2$  treatment had no significant effect on structural properties. On the other hand, optical transmittance of the films decreased after  $\text{CuCl}_2$  treatment. Also,  $\text{CuCl}_2$  treatment resulted in a very slight decrease in band gap energy. Photoelectrochemical performance of CdS thin films was investigated at room temperature and under  $35 \text{ mW/cm}^2$  illumination. Power efficiency of thin films increased dramatically after  $\text{CuCl}_2$  treatment. The maximum power efficiency obtained in this study was about 2%. Mott-Schottky analysis indicated that the samples are n-type and donor density

of treated samples is higher than as-deposited samples. Finally, frequency depended measurements showed that charge transfer mechanisms of  $\text{CuCl}_2$  treated samples was controlled by both kinetic and diffusion.

In addition to the deposition and characterization of CdS thin films, in this study, an electrochemical route for deposition of PPy and PPy/CdS thin film on ITO-PET substrate was utilized. Two absorption peaks for PPy films was observed around 390 and 590 nm on ITO-PET. The band gap energy of the PPy films determined from UV-vis analysis was about 2.0 eV. Fill factor and power efficiency of the PPy films increased after CdS deposition. The maximum power efficiency obtained in this study was 0.58%. This was one of the highest values for the polymeric PEC solar cells reported in literature. Frequency dependent measurements have also been performed. Mott-Schottky plots of PPy films showed that samples deposited for 5 min were p-type and the others were n-type. Hence, it is possible to mention about a p-n junction formation between PPy-5 min/CdS thin film electrodes. The magnitude of the band bending was about 0.7 V for this sample. Nyquist analysis of the thin films indicated that charge transfer in almost all samples was controlled by mixed diffusion and kinetic. Finally, Bode plots of samples revealed that charge transfer resistance of investigated thin films decreased with both CdS deposition and with the increase in the frequency.

## REFERENCES

1. Moss, S.J.; Ledwith, A. The Chemistry of the Semiconductor Industry, NEWYORK, Blackie&Son, **1987**, pp 2.
2. Giancoli, D. C. Physics for Scientists&Engineers with Modern Physics, Prentice Hall, **2000**, pp 1048.
3. Roulston, D. J. An Introduction to the Physics of Semiconductor Devices, Oxford University Press, **1999**, pp 5.
4. Fishbane, Gasiorowicz, Thornton, Physics for Scientists&Engineers with Modern Physics, Prentice Hall, **2005**, pp 1187-1193.
5. Dimitrijević, S. Principles of Semiconductor Devices, Oxford University Press, **2006**, pp 13.
6. Kakani S. L. Modern Physics, Anshan, **2007**, pp 1016-1026.
7. Fishbane, Gasiorowicz, Thornton, Physics for Scientists&Engineers with Modern Physics, Prentice Hall, **2005**, pp 1190-1191.
8. Rideneour, L. N. Modern Physics for the Engineer, McGraw-Hill, **1954**, pp 402.
9. Dimitrijević, S. Principles of Semiconductor Devices, Oxford University Press, **2006**, pp 187-199.
10. Chopra, K. L. Thin-Film Phenomena, McGraw-Hill, New York, **1969**.
11. Hegedus, S. Progress in Photovoltaics : Research and Applications, **2006**, Vol 14, pp 393-411.
12. Shi, Z.; Wenham, S. R.; Progress in Photovoltaics : Research and Applications, **1994**, Vol.2, pp 153-162.

13. Carlson, D. E. U.S Patent, **1977**, 4, 064, pp 521.
14. Ramanathan, K.; Contreras, M.; Perkins, C.; Asher, S.; Hasoon, F. Progress in Photovoltaics **2003**, 11, pp 225-230.
15. ROCKETT, A. The Materials Science of Semiconductors, Springer, **2008**, pp 395.
16. Yu, G.; Srdanov, G.; Wang, H.; Cao, Y. *J. Heeger, Proc.SPIE*, **2000**, 3929, pp 118–125.
17. Tang, C.W.; Van Slyke, S.A. *Appl.Phys.Lett.* **1987**, 51, pp 913–915.
18. Torsi, L.; Cioffi, N.; Di Franco, C.; Sabbatini, L.; Zambonin, P. G.; Blev-Zacheo, T. *Solid State Electron.* **2001**, 45, pp 1479–1485.
19. Drury, C. J.; Mutsaers, C.M.J.; Hart, C.M.; Matters, M.; de Leeuw, D.M.; *Appl.Phys. Lett.* **1998**, 73, pp 108–110.
20. Rockett, A. The Materials Science of Semiconductors, Springer, **2008**, pp 396-403.
21. Bidan, G. *Sensors and Actuators B*, **1992**, 6, pp 45-56.
22. Diaz, A.F.; Gardini, G.P.; Gill, W.D.; Grant, P.M.; Kanazawa, K.K.; Kwak, J.F.; Street, G.B. *Synth. Met.* **1980**, 1, pp 329.
23. Altgeld, W. in: F. Beck (Ed.), GDCh-Monographs, vol. 5, Elsevier Science Publisher, Frankfurt, **1996**, pp 552.
24. Wessling, B. *Synth. Met.* **1995**, 85, pp 1313.
25. Romeo, A.; Bätzner, D. L.; Zogg, H.; Tiwari, A. N.; Potential of CdTe thin film solar cells for space applications, 17th European Photovoltaic Conference and Exhibition, **2001**.

26. Zweibel, K.; Ullal, H. S.; and von Roedern, B. Photon International Publishing and Editorial Office, Solar Verlag GmbH, Aachen, Germany, **2004**, p. 4.
27. Çiçek B. N.; Öztürk M.; Özek N. *Renewable and Sustainable Energy Reviews*, **2009**, 13, pp 1428–1436.
28. Irvine, S.J.C.; Barrioz, V.; Lamb, D.; Jones, E.W.; Rowlands-Jones, R. L.; *Journal of Crystal Growth* **2008**, 310, pp 5198–5203.
29. Tarrant, D. E.; and Gay, R. R.; (Paper presented at Proc. 3rd World Conf. on Photovoltaic Energy Conversion, Osaka, **2003**).
30. Nakada, T.; Kume, T.; Mise, T.; Kunioka, A.; Japan Journal of Applied Physics **1998**, 37:, pp 499.
31. Ramanathan, K.; Contreras, M. A.; Perkins, C. L.; Asher, S.; Hasoon, F. S.; Keane, J.; Young, D.; Romero, M.; Metzger, W.; Noufi, R.; Ward, J.; Duda, A. *Progress in Photovoltaics Research and Applications*, **2003**, 11, pp 225-230.
32. Bodegard, M.; Stolt, L.; Hedstrom, J.; Proceedings of the 12th European Photovoltaic Solar Energy Conference, **1994**, 743–1746.
33. Bonnet, D.; Meyers, P.; *J. Mater. Res.* **1998**, 13, pp 2740.
34. Bonnet, D. *Thin Solid Films*, **2000**, 547, pp 361–362.
35. Kaur, I. J.; Pandya, D. K.; Chopra, K. L. *Journal of the Electrochemical Society*, **1980**, 127, pp 943.
36. Pandya, D.K.; Chopra, K.L. *Physics of Thin-Films*. Volume 11: Chemical Solution Deposition of Inorganic Films, Hass G (ed.). Academic Press: New York, **1980**.

37. Petritsch, K. Organic Solar Cell Architecture Thesis submitted to Technisch-Naturwissenschaftliche Fakultät der Technischen Universität Graz, Austria, **2000**.
38. Wada, T.; Kohara, N.; Negami, T.; Nishitani, M. *Japan Journal of Applied Physics*, **1996**, 35, pp 1253–1256.
39. Rorlevi, O.; Dobson, K.D.; Rose, D.; Hodes, G.; *Thin Solid Films*, **2001**, 387: 155–157.
40. Schuegraf, K.K. editor, Handbook of Thin-film Deposition Processes and Techniques, Noyes, **1988**.
41. Adams, A.C. VLSI Technology, McGraw-Hill, New York, **1983**, pp 93-129.
42. Robinson, McD.; Brekel, C.H.J.; Cullen, G.W.; Blocher, J.M. *Proc. Ninth. Internatl. Conf. On Chemical Vapor Deposition*, New Jersey, **1984**, Proc.Vol. 84-6.
43. Parker, E.H. editor, The Technology and Physics of Molecular Beam Epitaxy, Plenum Press, New York, **1985**.
44. Chang, L.L.; Ploog, K. editors, Molecular Beam Epitaxy and Heterostructures, Martinus nijhoff Publishers, Dordrecht/Boston/Lancaster, **1985**.
45. Bode, D.E.; Hass, G.R.E.Thun, editors, Physics of Thin Films, vol.3, Academic Press, New York, **1966**, pp.275.
46. Ojha, S.M.; Hass, G.; Francome, M.H.; Vosses, J.L. editors, *Phys.of Thin Films*, Vol. 12, Academic Press, New York, **1982**, pp 237-296
47. Wolf, H.F. Semiconductors, Wiley, New York, **1971**, pp 342-362.
48. LEE, J.-H. *Thin Solid Films*, **2007**, 515: 6089-6093.

49. Romeo, N.; Bosio, A.; Canevari, V. *Proceedings of Third World Conference on Photovoltaic Energy Conversion*, WCPEC-3, **2003**, Vol 1, pp 469-470.
50. Frekides, C.S.; Ceekala, V.; Dugan, K.L.; Killian, Oman, D.M.; Swaminathan, R.; Morel, D.L. *Proceedings of AIP Conference*, **1995**, No. 353, pp 39-45.
51. Romeo, A.; Batzner, D.L.; Zogg, H.; Vignali, C.; Tiwari, A.N. *Solar Energy Materials & Solar Cells*, **2001**, 67, pp 311-321.
52. Romeo, A.; Batzner, D.L.; Zogg, H.; Tiwari, A.N. *Thin Solid Films*, **2000**, 361, pp 420-425.
53. Kobayashi, M.; Kitamura, K.; Umeya, H.; Jia, A. W.; Yoshikawa, A.; Shimotomai, M.; Kato, Y.; Takahashi K. *J. Vac. Sci. Technol.* , **2000**, 18-3, pp 1684-1687
54. Khrypunov, G.; Romeo, A.; Kurdesau, F.; Batzner, D.L.; Zogg, H.; Tiwari, A.N. *Solar Energy Materials & Solar Cells*, **2006**, 90, pp 664-677.
55. Kitaev, G.A.; Uritskaya, A.A.; Morkrushin, S.G. *Russ. J. Phys. Chem.* , **1965**, 39, pp 1101.
56. Kaur, I.; Pandya, D.K.; Chopra, K.L. *J. Electrochem. Soc.* , **1980**, 127, pp 943.
57. Choi, J.; Kim, K.-J.; Ypp, J.-B.; Kim, D. *Solar Energy*, **1998**, 64, pp 41.
58. Premaratne, K.; Akuranthilaka, S.N.; Dharmadasa, I.M.; Samantilleka, A.P. *Renew. Energy*, **2003**, 29, pp 549.
59. Kolhe, S.; Kuljarni, S.K.; Nigavekar, A.S.; Sharma, S.K. *Sol. Energy Mater.* , **1984**, 10, pp 47.
60. Kaur, I.; Pandya, D.K.; Chopra, K.L. *J. Electrochem. Soc.* , **1980**, 127, pp 943.

61. Danaher, W.J.; Lyons, L.E.; Morris, G.C. *Sol. Energy Mater.* , **1985**, 12, pp 137.
62. Lee, J-H. *Thin Solid Films*, **2007**, 515, pp 6089-6093
63. Baranski, A.S.; Fawcett, W.B. *J. Electrochem. Soc.* , **1980**, 127, pp 766.
64. Tan, W.; Chen, J.; Zhou, X.; Zhang, J.; Lin, Y.; Li, X.; Xiao, X. *J Solid State Electroche.*, **2009**, 13, pp 651.
65. Mathew, X.; Enriquez, J.P.; Romeo, A.; Tiwari, A.N. *Sol. Energy*, **2004**, 77, pp 831.
66. Semenikhin, O.A.; Ovsyannikova, E.V.; Alpatova, N.M.; Rotenberg, Z.A.; Kazarinov, V.E. *J Electroanal. Chem.* , **1999**, 463, pp 190.
67. Gazotti, W.A.; Nogueira, A.F.; Giroto, E.M.; Gallazzi, M.C.; Paoli, M.A.D. *Synth. Met*, **2000**, 108, pp 151.
68. Liu, P.; Chen, T.H.; Pan, W.Z.; Huang, M.S.; Deng, W.J.; Mai, Y.L.; Luan, A.B. *Chin. Chem. Lett.* , **2008**, 19, pp 207.
69. Grimes, C.A.; Dickey, E.C.; Pishko, M.V. editors, *Encyclopedia of Sensors*, American Scientific Publishers, California, **2006**.
70. Iroh, J.O.; Su, W. *Electrochim. Acta.* , **2000**, 46, pp 15.
71. Scrosati, B. *J. Electrochem. Soc.* , **1989**, 136, pp 2774.
72. Nagai, H.; Segawa, H. *Chem Commun.* , **2004**, 8, pp 974.
73. Zhang, Z.; Yuan ,Y.; Liang, L.; Cheng, Y.; Xu, H.; Shi, G.; Jin, L. *Thin Solid Films*, **2008**, 516, pp 8663.
74. Hao, Y.; Yang, M.; Li, W.; Qiao, X.; Zhang, L.; Cai ,S. *Sol. Energy Mater. Sol. Cells.* , **2000**, 60, pp 349.

75. Fujii, M.; Abe, S.; Ihori, H. *Synth. Met.* , **2005**, 152, pp 41.
76. Martins, N.C.T.; Silva, M.T.; Montemora, M.F.; Fernandes, J.C.S., Ferreira, M.G.S. *Electrochim. Acta.* , **2008**, 53 , pp 4754.
77. Otabatmaz, G., M.S. Thesis, Middle East Technical University, Ankara, Turkey, **2002**.
78. He, Z.; Zhao, G.; Weng, W.; Du, P.; Shen, G.; Han, G.; *Vacuum*, **2005**, 79, pp14.
79. Lee, J-H.; Lee, D-J. *Thin Solid Films*, **2007**, 515, pp 6055.
80. Nanda, K.K.; Sarangi, S.N.; Sabu, S.N. *Nanostruct Mater.*, **1998**, 10, pp 1401.
81. Hur, S-G.; Kim, E-T.; Lee, J-H.; Kim, G-H.; Yoon, S-G. *J. Vac. Sci. Technol.* , **2008**, B 26:4, pp 1334.
82. Nizamoglu, S.; Mutlugun, E.; Akyuz, O.; Kosku Perkgoz, N.; Demir, H. V.; Liebscher, L.; Sapra, S.; Gaponik, N.; Eychmüller, A. *New. J. Phys.*, **2008**, 10, 023026.
83. Kokate, A.V.; Asabe, M.R.; Hankare, P.P.; Chougule, B.K. *J. Phys. Chem. Solids*, **2007**, 68, pp 53.
84. Rincon, M.E.; Martinez, M.W.; Miranda-Hernandez, M. *Thin Solid Films*, **2003**, 425, pp127–134.
85. Lade, S.J.; Uplane, M.D.; Lokhande, C.D. *Materials Chemistry and Physics*, **2001**, 68, pp 36–41.
86. Hilal, H. S.; Ismail, R.M.A.; El-Hamouz, A.; Zyoud, A.; Saadeddin, I. *Electrochim. Acta.* , **2009**, 54, pp 34-33.

87. Refczynska, M.; Mieczkowski, J.; Skompska, M. *Electrochim. Acta.* , **2008**, 53, pp 29-84.
88. Martirosyan, S. *Sol. Energ. Mat. Sol. C.*, **2001**, 70, pp 115.
89. Barsoukov, E.; Macdonald, J. R.; Impedance Spectroscopy, Second Edition, John Wiley & Sons Inc., **2005**, pp 296-302
90. Barsoukov, E.; Macdonald, J. R.; Impedance Spectroscopy, Second Edition, John Wiley & Sons Inc., **2005**.
91. Oh, E.J.; Jang, K.S.; Su, J.S.; Kim, H.; Kim, K.H.; Yo, C.H.; Joo, *J. Synth. Met.*, **1997**, 84, pp 147.
92. Kim, H.; Chang, W. *Synth. Met.* , **1999**, 101, pp 150.
93. Harris, C.J.; Belcher, W.J.; Dastoor, P.C. *Sol. Energy Mater. Sol. Cells* , **2007**, 91, pp1127.
94. Sikora, E.; Macdonald, D.D. *Electrochim. Acta*, **2002**, 48-1, pp 69-77
95. Bard, A.J.; Faulkner, L.R. *Electrochemical Methods: Fundamentals and Applications*. Wiley, New York, **1980**.
96. Grant, C.D.; Schwartzberg, A.M.; Smestad, G.P.; Kowalik J.; Tolbert, L.M., Zhang, J.Z, *Synth. Met.* , **2003**, 132, pp 197.
97. Tuken, T. *Surf. Coat. Technol.*, **2006**, 200, pp 4713.